NAS8-36655

REPORT

FINAL

PHASE II - LUBRICANT EVALUATION OF THE ALPHA AND BETA JOINTS

To

NASA Marshall Space Flight Center

February 12, 1992

Battelle
. . . Putting Technology To Work

Functional Color Pages 1

	Monthly Progress Report	Final Progress Report	Final Progress Draft	Financial Management Report
NASA Marshall Space Flight Center Attn: Marshall Space Flight Center, AL 35812				
AP52-F	1**	0*	1**	1
CN22D	3	0	5	0
AT01	1	0	1	0
BF30	0	0	1	1
CC01/Wofford	1	1	1	0
EM13B-21	1	0	1	1
KA02	1	0	1	1
EH14/Fred Dolan	5 + repro	2	10 + repro	1
NASA Scientific and Technical Information Facility Attn: Accessioning Department P.O. Box 8757 Baltimore/Washington International Airport, Maryland 21240	1 + repro	0	1 + repro	0
Robert Acres Mail Stop ES-62 Lyndon B. Johnson Space Flight Ctr. Houston, TX 77058-3696				
Dr. Mike Gardos Hughes Aircraft Corporation Mail Stop F150 P.O. Box 902 El Segundo, CA 90245				

Phase II Final Report
Contract NAS8-36655

on

Lubricant Evaluation of the Alpha and Beta Joints

to

NASA Marshall Space Flight Center
Marshall Space Flight Center, Alabama 35812

February 12, 1992

by

J.W. Kannel
R.D. Stockwell

BATTELLE
505 King Avenue
Columbus, Ohio 43201-2693

TABLE OF CONTENTS

LIST OF FIGURES

LIST OF FIGURES (Cont).

PAGE

LIST OF TABLES

PAGE

SUMMARY

A research study was conducted to evaluate dry film lubrication of long life space components such as the Alpha and Beta joints of the Space Station. The problem addressed in the report pertains to the longevity of sputtered MoS_2 or ion plated lead films in a rolling contact environment. A special technique was devised for the experiments, which incorporated a coated ball cyclically loaded against a flat plate. At fixed intervals the surface of the coating was photographed at 100X magnification. By computer scanning the photographs, the rate of coating loss was determined. Experimental variables included load and surface finish of the plate.

A theory was developed to analyze the state of stress between ball and flat. The stress condition in the ball apparatus was related to the state of stress under rolling contact conditions. Based on the experiments life appeared to decrease with increasing load and increasing surface roughness. An ion plated lead film gave better life than a sputtered MoS_2 film. However, by keeping the interfacial shear stress at a low level, adequate coating life was achieved for either coating. For the MoS_2 film the critical stress was found to be about 0.055 GPa (8 ksi). For the lead film, the critical stress was about 0.19 GPa (28 ksi). The study dealt only with mechanical wear. Before a coating is selected for a critical space application other factors such as reaction with atomic oxygen must also be considered.

NOMENCLATURE

b	Half width of contact
b_o	Half width of Hertzian contact
E	Young's modulus
h	Coating thickness
p	Pressure
p_c	Contact pressure distribution
p_f	Pressure distribution due to contact of one body with a rigid flat
p_H	Maximum Hertzian pressure
R	$1/R_1 + 1/R_2$
R_1, R_2	Radii of contacting bodies
s	$h\omega$
u	Deflection in direction of x coordinate
v	Deflection in direction of y coordinate
w'	Load (per unit length)
x	Coordinate variable
y	Coordinate variable
Δx	Increment on x
η	y/h
υ	Poisson's ratio
ϕ	Influence coefficient relating pressure to tangential deformation
ψ	Airy's stress function
σ	Normal Stress
τ	Shear stress
ω	Variable used in Fourier Transform

Phase II Final Report
Contract NAS8-36655

on

Lubricant Evaluation of the Alpha and Beta Joints

to

NASA Marshall Space Flight Center
Marshall Space Flight Center, Alabama 35812

by

J.W. Kannel
R.D. Stockwell

BATTELLE
505 King Avenue
Columbus, Ohio 43201-2693

INTRODUCTION

A major life-limiting factor for spacecraft mechanisms is the lubrication system. In components such as the Alpha and Beta joints of the Space-Station, dry film unreplenishible lubricants will likely be required. Although such coated films can give very good performance life, they will eventually wear away. Therefore, efforts must be made to optimize factors such as the type of coating, surface roughness, and contact stress imposed on the coatings.

A technique was developed for evaluating coating life in an Alpha or Beta joint application. The technique consists of cyclicly loading a coated ball against a flat and of measuring the loss of coating from the ball. The flat can be smooth or rough. Photographs of the ball are taken after various load-cycle intervals. The photographs are analyzed using a computer scanner and the ratio of bare steel (i.e. depleted coating) to coated steel is computed. Coating loss is plotted as a function of loading cycles.

Theoretical analyses were conducted to relate the stress-slippage conditions in a ball-flat experiment to the condition in a bearing. The analyses relate load between the ball and flat to tangential deflection of the interface and subsequently to interfacial shear stresses. By this approach the experimental data can be extrapolated to rolling contact situations.

The report discusses the basic requirements of the Alpha and Beta joints based on discussions with Rocketdyne and Lockheed personnel. The report also describes the coating wear tests and analytical data for MoS_2 and ion-plated lead coatings. Based on the data analyses, suggestions for candidates for Alpha and Beta joint lubricants based on mechanical wear are given.

ALPHA AND BETA JOINT TRIBOLOGY NEEDS

Solar Alpha Joint

Figure 1 is an illustration of the Solar Alpha Rotary Joint (SARJ) for Space Station (from Lockheed). The SARJ is the rotating connector between the main Space-Station assembly and the solar power assembly panel. The joint must rotate 360 degrees for each orbit of the Space Station (~ 90 minute period). Figure 2 shows a scaled-down test configuration being evaluated by Lockheed. The design consists of a series of 16 support roller assemblies (3 rollers per assembly) loaded against a ring-rail. The bearing (ring-rail) diameter will be on the order of 3.66 m (12 feet); the support rollers will be about 0.06 (2.5 inches) in diameter. The rollers will be supported in special needle roller bearings that contain thrust washers (made from Kahrlon) to absorb axial loads on the rollers.

In general the roller preloads need not be excessive and the required number of load cycles is relatively small (compared with conventual bearing contacts). The SARJ itself must endure only about 175,000 cycles over a 30-year time period, and the rollers must operate for about 10^7 cycles. Roller-rail loading would be expected to be on the order of 87 kN/m (500 lbs/in). The primary load requirement pertains to the start-up torque on the SARJ.

The SARJ will be rotated through a ring gear with teeth integral with the ring-rail assembly. The gear system must be capable of transmitting extremely high torques 271 Nm (~ 2400 ft-lbs) during start-up. Operating torque would be significantly less than start-up; torque estimates are of on the order of 135 Nm (1200 ft-lbs). Despite the high torque levels the actual power requirements are very small because of the low rotational speed. For example, a 135 Nm (1200 ft-lb) torque with 1 revolution per 90 minutes corresponds to 1.9 watts (0.0025 HP).

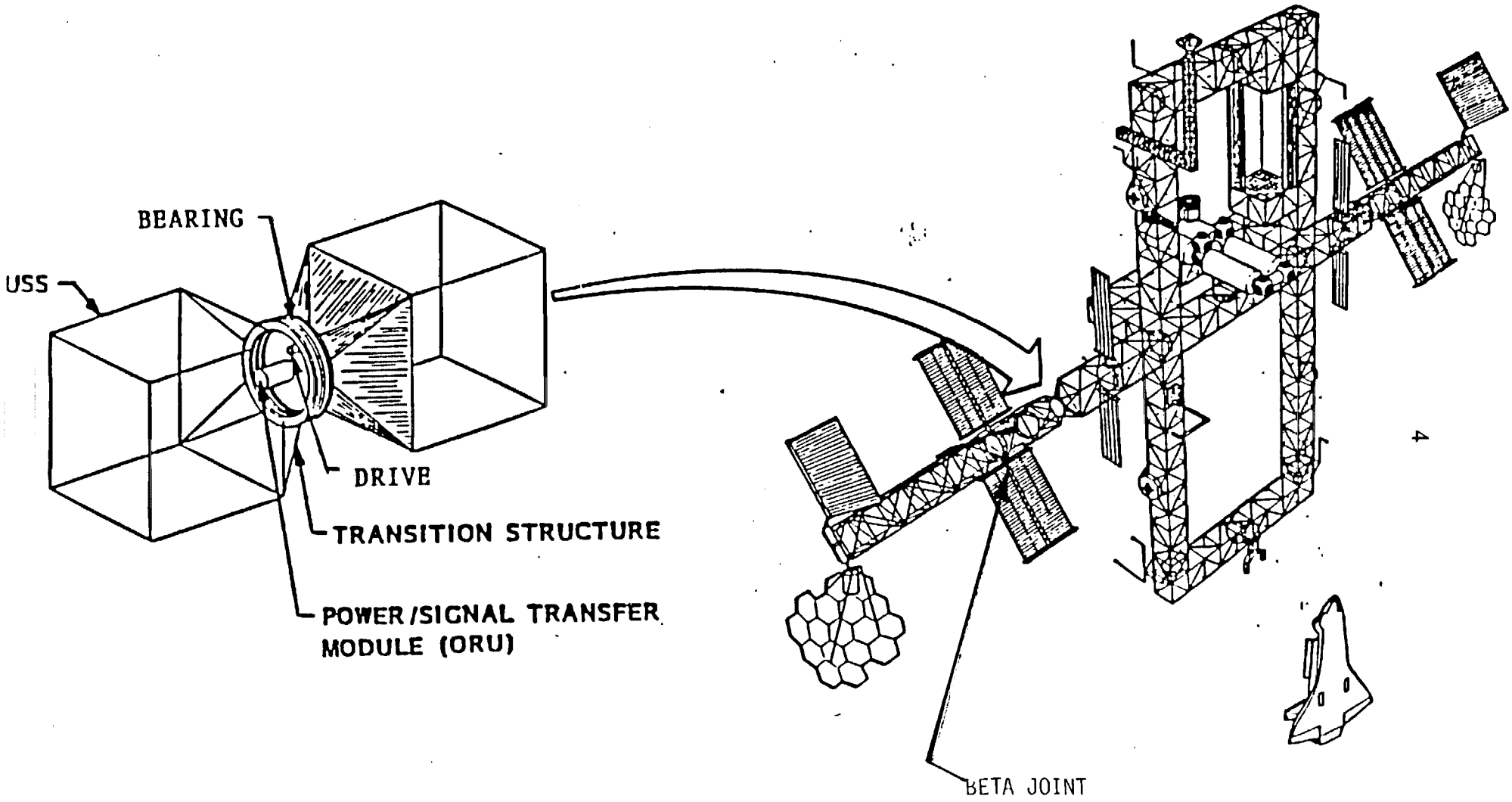

FIGURE 1. ILLUSTRATION OF ALPHA JOINT (LOCKHEED)

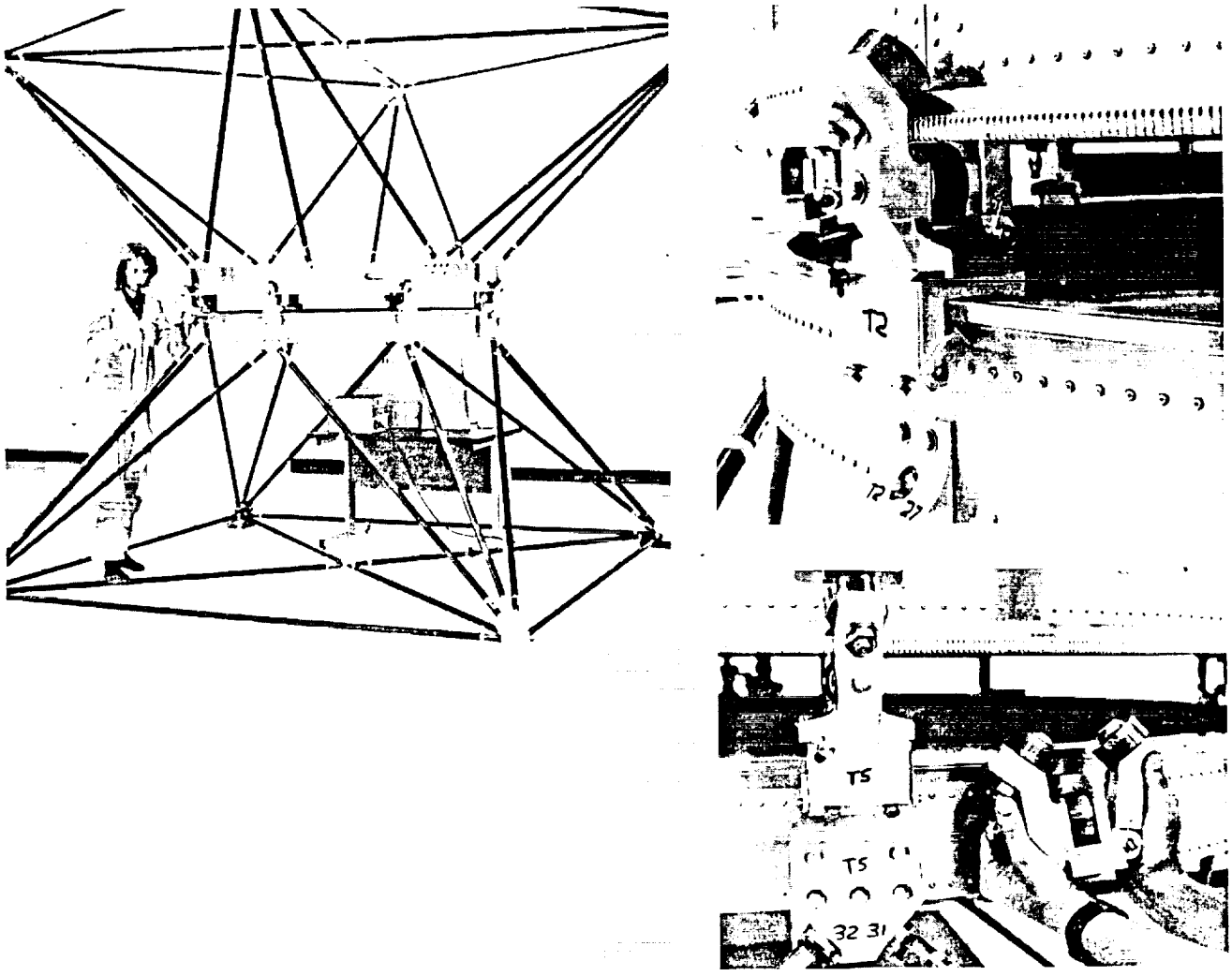

FIGURE 2. ALPHA JOINT TEST CONFIGURATION (LOCKHEED)

The Beta Joint

Figure 3 shows an illustrative drawing of the Beta joint. This joint forms the connection to the solar panel arrays. The solar panels will be on the order of 30 m (100 feet) by 9 m (30 feet). The Beta joint will oscillate (dither) at a rate of ± 0.9 degrees/minute and must be capable of larger angle oscillations (~ ± 60 degrees) under anomalous conditions.

The normal and radial loads on the Beta joint are only a nominal ± 1330 N (300 lbs); however, the bending moment and torsional moment can be large (on the order of ± 5600 Nm (50,000 in-lb) and 790 Nm (7000 in.-lb), respectively). The development of the Beta joint is currently in the design phase and an official concept has not been released. The Beta joint will likely use two or more roller (or cross roller) bearings with about a 0.25 m (10-inch) diameter shaft.

Components of Concern

Both the Alpha and the Beta joints have several interfaces that need tribological considerations. Components of concern are summarized in Table 1 and discussed below.

1. **SARJ Main Bearing Rail.** The rail is in rolling contact with three support rollers. The rail roller interfaces will probably be lubricated with a dry film such as molybdenum disulfide (MoS_2). The roller surfaces can be coated by sputtering with MoS_2 in a vacuum chamber. However, because of its size, the rail would be awkward to sputter and a more conventionally bonded film may be more tenable.

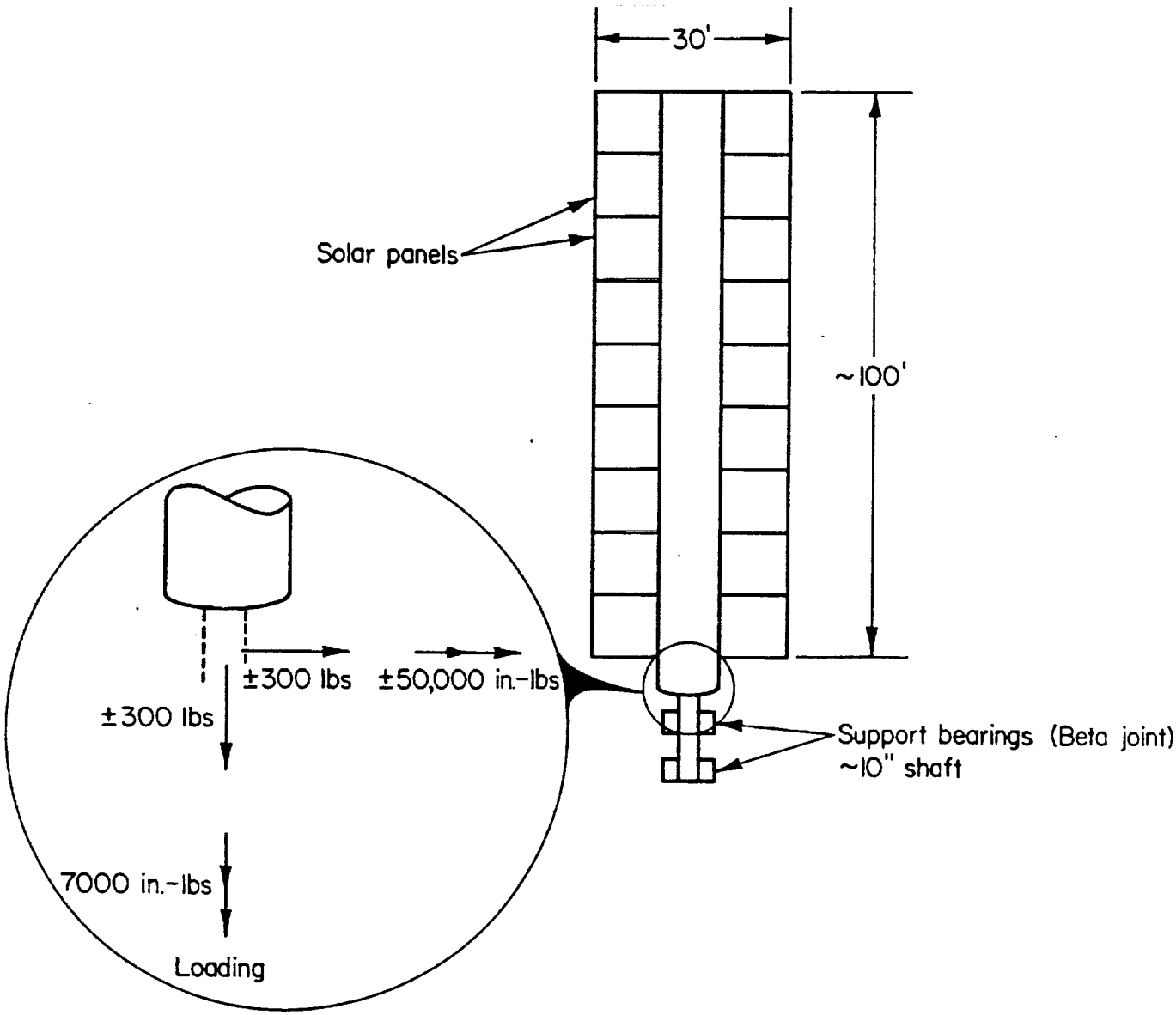

FIGURE 3. ILLUSTRATION OF BETA JOINT (ROCKETDYNE)

TABLE 1. SUMMARY OF POSSIBLE TRIBOLOGICAL COMPONENTS FOR ALPHA AND BETA JOINTS

Assembly	Component	Elements	Possible Material	Possible Lubricants
1. Alpha Joint	Main bearing	Rail	Stainless Steel, Titanium	None, bonded films
2. "	"	Roller surface	Stainless Steel	Sputtered MoS_2
3. "	"	Roller-support bearing	Stainless Steel	Grease (BRAY)
4. "	Ring gear	Output pinion	Stainless Steel	Grease, bonded film
5. "		Motor pinion		Grease
6. "	"	Support bearings		Grease
7. Beta joint	Support system	Gimbal bearing	Stainless Steel	Sputtered films

2. **SARJ Roller Support Bearings.** The rollers will be supported by needle (possibly self aligning) bearings. The bearings will probably be lubricated with a low outgassing grease such as Braycote 601. Since grease lubricated bearings are well within the state-of-the-art, no general tribology efforts should be required except for life testing.

3. **SARJ Roller Support Bearings.** The current roller bearings concept contains a Kahrlon thrust washer, which introduces high friction into the bearing. Materials and designs that may yield lower friction should be considered.

4. **SARJ Output Pinion Gear.** One of the most critical tribological interfaces is between the meshing gear teeth of the drive system. The interface could be grease lubricated, although a dry contact would be preferred to minimize outgassing.

5. **SARJ Motor Pinion.** The motion pinion gear will probably be in a vented chamber and most likely will be grease lubricated. No unusual tribological problem would be expected. Life testing should be conducted by the major contractors.

6. **SARJ Motor Support Bearings.** The bearings will probably be grease lubricated. Bearing life tests should be conducted.

7. **Beta Joint Gimbal Bearing.** The Beta joint possesses some difficult tribological problems because of the high moments and oscillatory motion. This type of motion can result in fretting damage to the bearing and resulting torque irregularities. The bearings will probably be dry film lubricated. Data are needed to establish coating life, bearing jamming due to coating migration, and coating load limitations.

A survey of lubricants for applications such as those on Space Station was the focus of the Phase III report of the contract. The survey discusses liquid and dry lubricants that are readily available and that have been used in space applications. A primary concern for the Alpha and Beta joints is the coating on the rollers, which will be an important aspect of design and evaluation. The primary concern is coating durability, which is related to:

- Coating type,
- Loading, and
- Surface roughness.

The remainder of this document focuses on theoretical and experimental research in coating performance.

BALL-FLAT COATING WEAR TEST

Testing Technique

The technique used in the solid lubricating film evaluation tests is illustrated in Figure 4. A coated 12 mm (0.5 inch) diameter Type 440C ball was loaded against a flat steel plate (smooth or rough). The ball contained surface coatings (sputtered MoS_2 or ion plated lead) to be evaluated. The ball holder was in contact with a loading spring that is driven by a special cam. The cam was rotated at 300 rpm, which imposed 600 load cycles on the ball per revolution. A standard roller follower (of the type used in diesel engines) was used to apply the cam motion to the spring. The load was varied between ten percent of full load and full load for each cycle.

A ground wire was soldered to the ball and the plate was electrically insulated from ground to allow for electrical continuity measurements across the MoS_2 coatings. The goal of the continuity experiments was to establish the continuity of the coating or more precisely the time the coating failed. However, quantifying the results of the continuity experiments was difficult because in some tests the coatings tended to appear to fail and then reheal due to material transfer from plate to ball. In the experiments reported here the coatings were evaluated based on periodic microscopic examinations of the ball surfaces.

Data Analysis

General Observations

Photographs were taken of the ball surface before the start of each test and several times during the course of the experiments. Most tests were conducted for about 200,000 (200K) cycles. Figure 5a shows typical photomicrographs for an MoS_2 coated ball after 302K cycles of testing. Figure 5b shows a photomicrograph of an ion plated lead coated ball after 360K cycles. For the MoS_2 coating there is an obvious zone in the center that contains a thick layer of the coated film. Outside the ring of good coating there is an obvious wear zone.

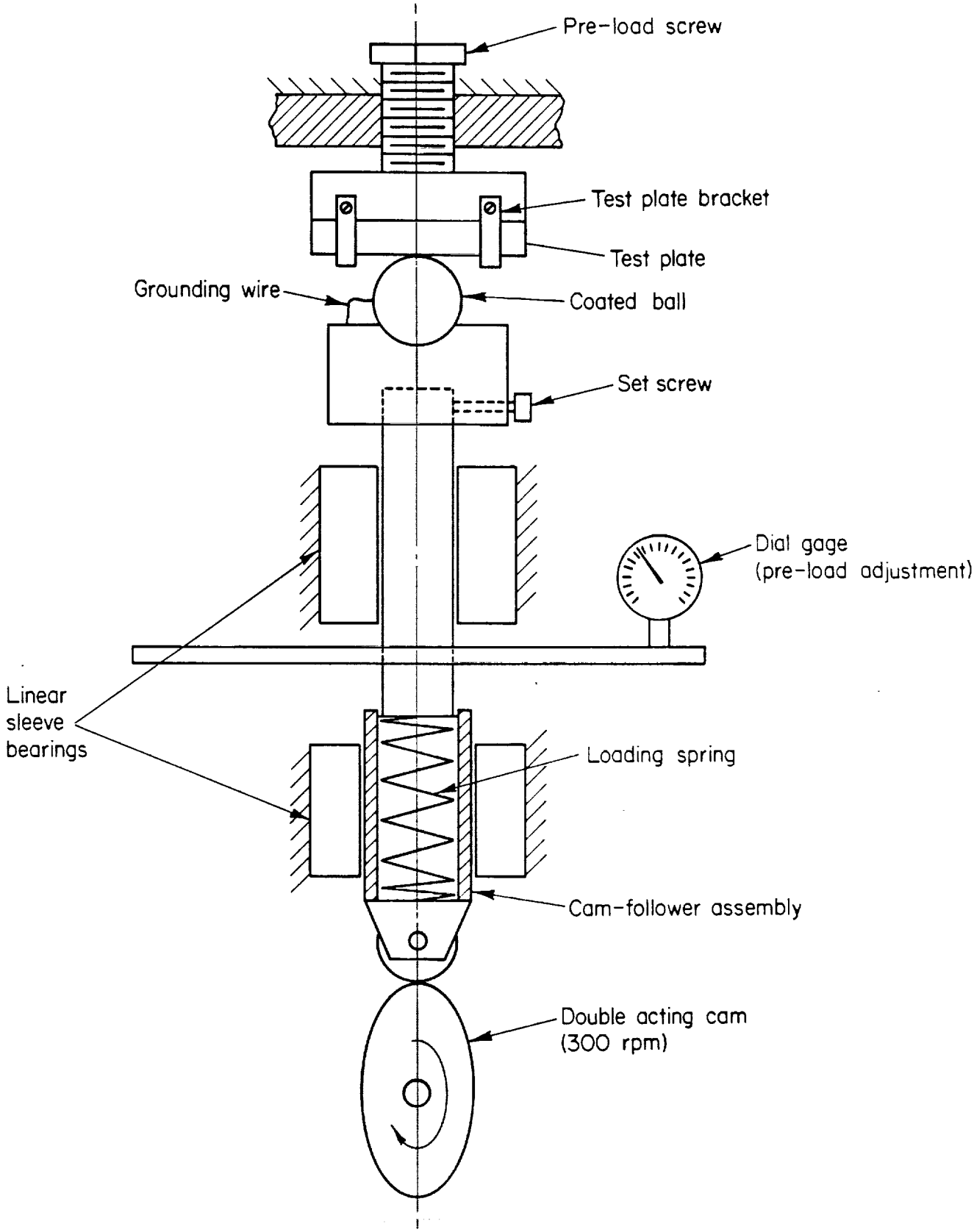

FIGURE 4. SCHEMATIC DRAWING OF TEST APPARATUS

Ball After 302K Cycles

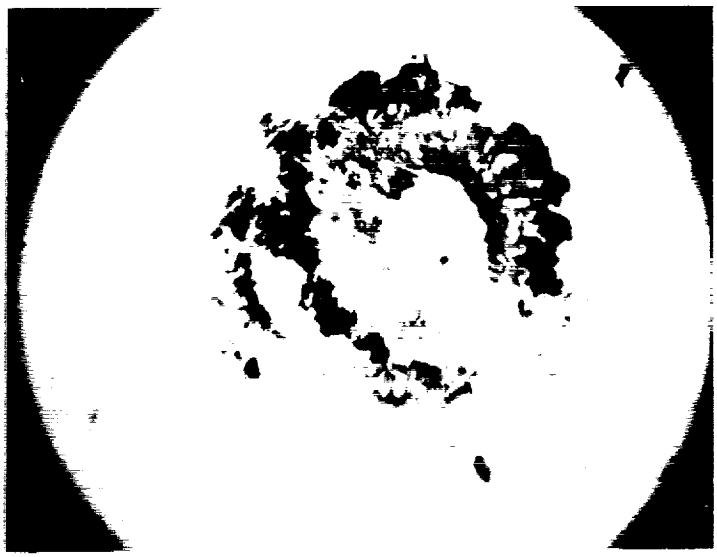

Plate After 40K cycles

a. MoS_2 Coating at 111 N (25 lbs) Load

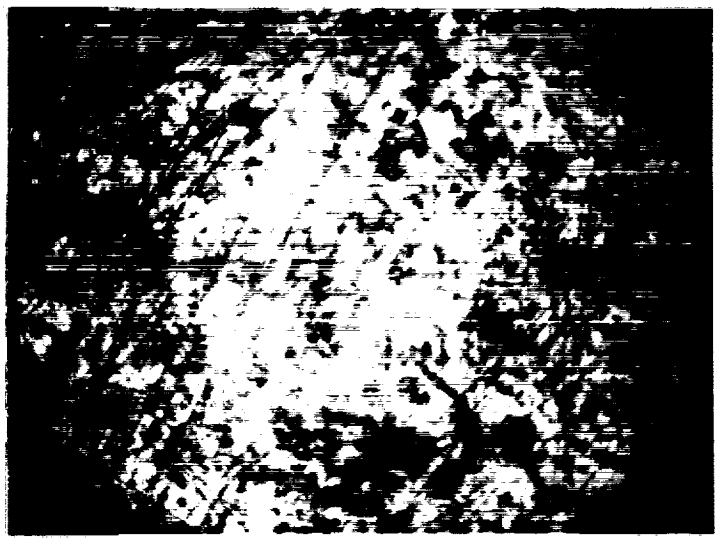

Ball After 360K Cycles

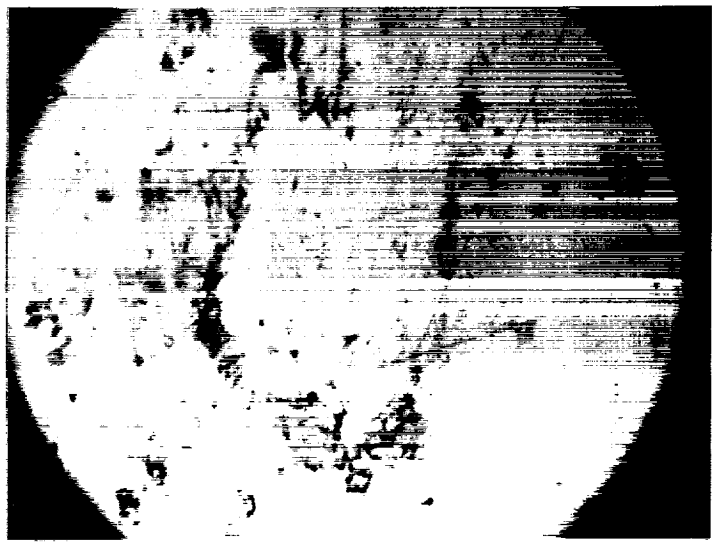

Plate after 360K cycles

b. Ion Plated Lead at 111 N (25 lbs) Load

FIGURE 5. TYPICAL PHOTOMICROGRAPHS OF BALL AND PLATES (100X)

Theoretically the center zone is a region of adhesion between ball and plate (see Figure 6). As the ball impresses the flat, interfacial shear stresses are usually generated*. The shear stresses are zero in the center of contact and rise sharply toward the edge. At some point the stresses are higher than the coefficient of friction times the local pressure and slippage occurs.

When the interfacial shear stress exceeds the adhesive strength of the coating to the substrate, coating failure can occur. The most likely region for such failures is the slip region of the interface. In the slip region surface asperities on the ball and flat move relative to each other and can create very high localized stress concentrations. These stress concentrations then will tend to chip the coating. The wear zone of Figure 5 is probably the slip region and the non-wear zone is probably the adhesive region.

Data Analysis Technique

A special technique was developed for analyzing ball-flat experiments for wear evaluations. The technique consisted of photographing the ball surface (at 100X magnification) at various time intervals and assessing the amount of steel exposed in the worn region as seen in the photographs. The data analyses were performed using a computer scanning technique.

A series of photographs taken after various numbers of cycles for a given test condition were scanned into a computer. The computer was then focused on the (theoretical) Hertzian contact zone of each photograph. Using a special software program (CTICA) the Hertzian region was scanned pixel by pixel and the ratio of white (coating-depleted points) to non-white (coating-intact points) pixels was computed. The ratio was used as an indication of coating loss.

---

*As discussed in the analyses section a major exception to this statement occurs when two balls of identical material are loaded together.

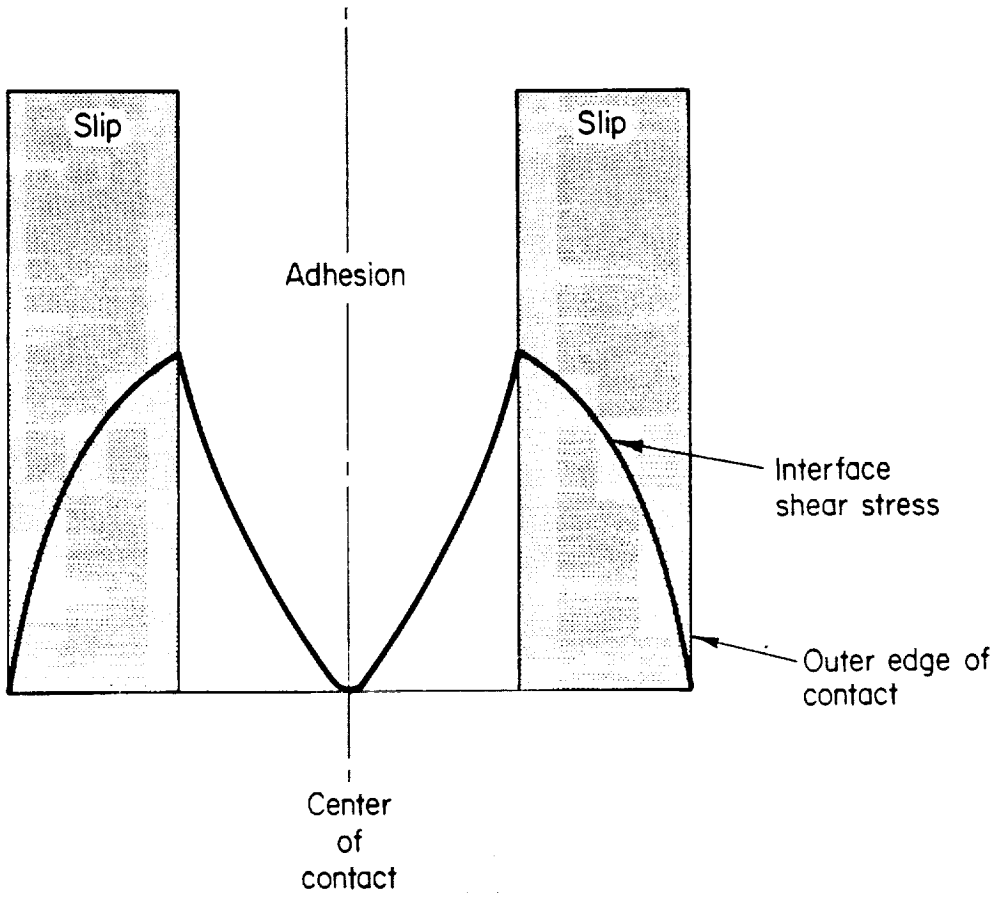

FIGURE 6. ILLUSTRATION OF SHEAR STRESSES BETWEEN BALL AND FLAT

Coating Wear Data

Molybdenum Disulfide Coating

Figure 7 presents coating wear as a function of number of cycles for two loads and two plate roughness conditions for a MoS_2 coating. Clearly the higher the load and the roughness the greater the coating wear. The coatings tended to wear rapidly in the initial cycles of testing but leveled out after about 10,000 cycles. Apparently MoS_2 coatings tended to transfer from ball to plate and eventually back to the ball. Photographs of the plate (Figure 5) clearly show MoS_2 transfer layers.

In large bearings such as the Alpha joint bearing, probably only the rollers would be coated. This coating would be transferred to the rings and would eventually be depleted from the rollers. Therefore for coating evaluation purposes the wear rate before transfer from the ball (i.e., during the initial cycles) is probably more representative of coating wear in the Alpha and Beta joints.

Ion Plated Lead Coatings

A plot of coating wear versus cycles for ion plated lead is shown in Figure 8. A photograph of a typical "worn" coating is given in Figure 5. In the lead coating tests, the wear rate tended to be much lower than for the MoS_2 coatings but also tended to occur more uniformly around the contact region rather than at the edges as seen with the MoS_2 coatings.

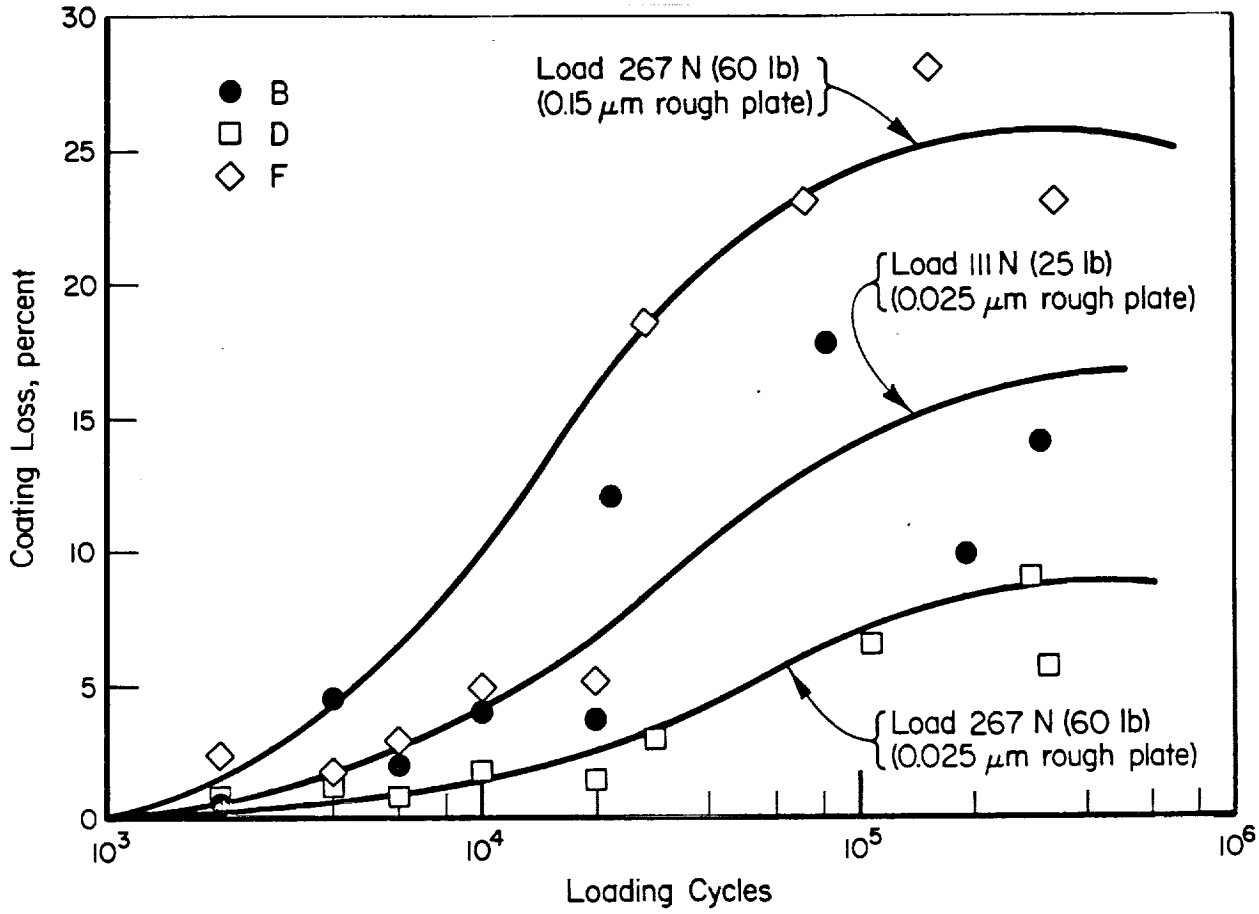

FIGURE 7. MoS_2 COATING LOSS IN BALL TEST APPARATUS

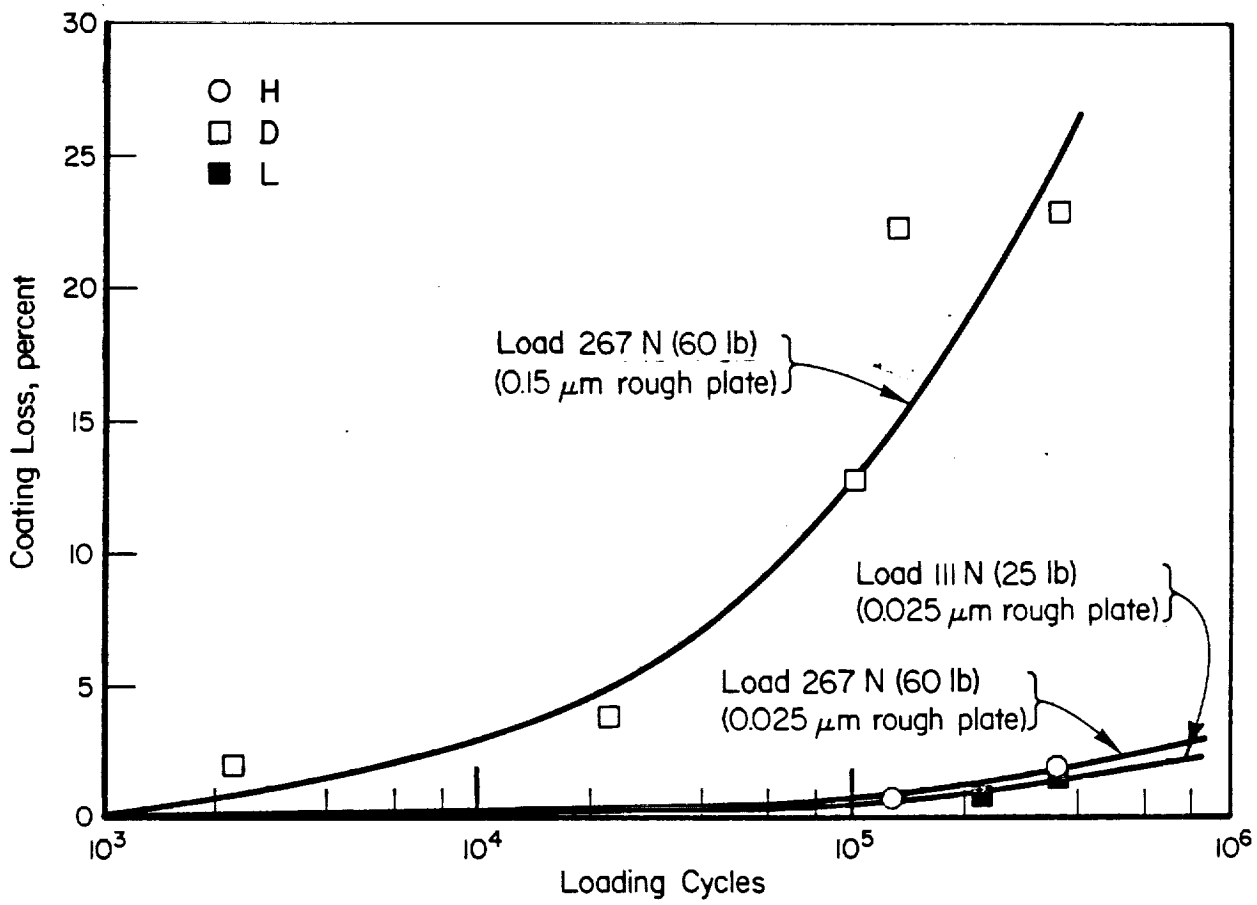

FIGURE 8. ION PLATED LEAD FILM COATING LOSS IN BALL TEST APPARATUS

ANALYSES OF SURFACE SHEAR FORCES IN COATED BODIES

When surfaces such as a ball and flat come into normal contact, their surfaces deform tangentially as well as in the normal direction. If both surfaces deform the same, such as could occur for the contact of two identical balls, no shear stress is developed. However, under most conditions a differential tangential deflection occurs, which produces surface shear stresses.

The surface shear is zero at the center of contact and rises rapidly away from the center (see Figure 6). At some point the surface shear is equal to the friction coefficient times the pressure. At this point slip occurs and surface damage can occur, especially to coatings. The purpose of the analysis was to develop equations for predicting interface tangential deflection and interfacial shear force to assist in designing long-life dry-film-lubricated contacts.

Tangential Deflection Due to Normal Load

Point Load

Consider the contact of two rollers of radius R_1 and R_2 as illustrated in Figure 9. As a result of this contact there is a movement u(x) of the surface of each roller, which depends on the specific modulus and radius of each roller as well as the applied load. Poritsky[1] gives the following expression for the deformation of a flat surface due to a point (elastic) load (Figure 10).

$$u = \begin{cases} -\dfrac{2(1+\nu)(1-2\nu)}{E} F_y & x>0 \\ +\dfrac{2(1+\nu)(1-2\nu)}{E} F_y & x<0 \end{cases} . \qquad (1)$$

E is Young's modulus and ν is Poisson's ratio. In essence Equation 1 says that on a flat surface a point load produces a constant positive deflection to the left of the load and a negative deflection to the right.

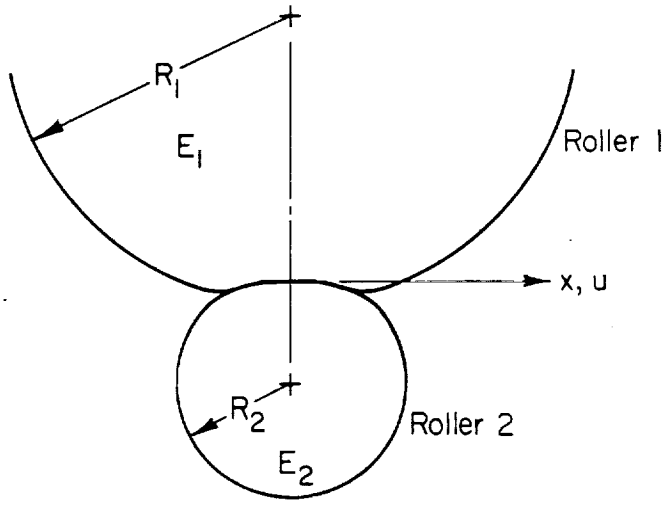

FIGURE 9. CONTACT OF TWO ELASTIC ROLLERS

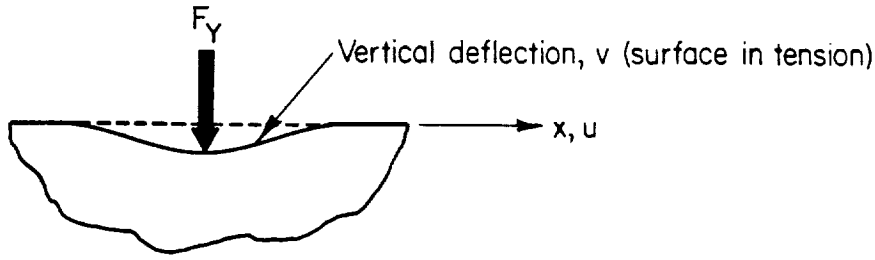

a. Positive Load Produces Vertical Deflection with Surface in Tangential Tension

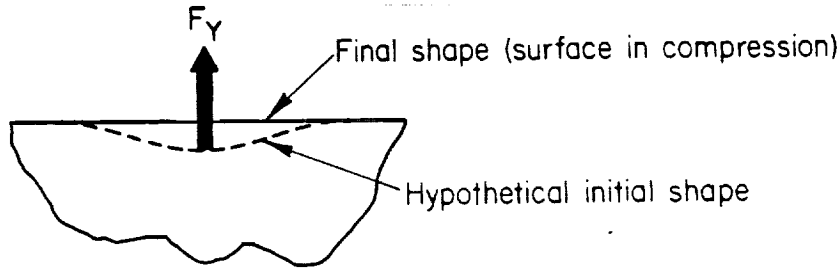

b. Negative Load Produces Flat Surface in Tangential Compression from Hypothetical Shape

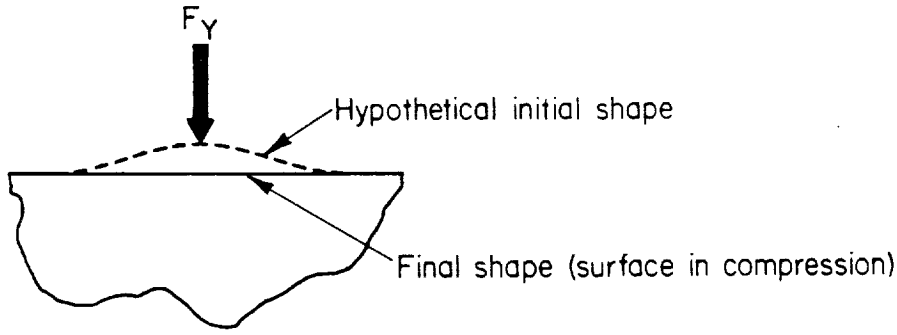

c. Positive Load on Curve Surfaces also Produce Flat Surface in Tangential Compression (U-negative)

FIGURE 10. POINT NORMAL LOAD ON A FLAT PLANE

The contact of curved surfaces is more complicated than occurs with a point load on a flat surface since the curve must be initially flattened. The force required to flatten the surface will produce deflections equivalent to that given by Equation 1 but in the opposite direction. To understand the equivalence consider the deflection shown in Figure 10a. If this deflection pattern was the initial shape of the surface, (Figure 10b or 10c), a load of F_y would flatten the surface. This load then would produce the same deflection as given by Equation 1 but with the opposite sign.

Effect of Distributed Load

The total tangential deflection of the surface could be:

$$u(i) = \sum_{j=1}^{n} \phi_1(i,j)\, p(j)\, \Delta x \ , \tag{2}$$

where ϕ_1 is the influence coefficient relating a normal unit load at point j to a tangential deflection at point i, and p(j) is the pressure at point j.

For the case shown in Figure 9, part of the interfacial pressure flattens Roller 1 and part of the pressure indents it beyond a flat surface. Let the pressure to flatten the surface be given by p_{F1} (j) and the pressure to indent the surface beyond the flat be given as $[p_c$ (j) - p_{F1} (j)]. The total deflection then is given as:

$$u_1(u) = \sum_{j=1}^{n} -\phi_1(i,j)\, p_{F1}(j)\, \Delta x + \phi_1(i,j)\, [p_c(j) - p_{F1}(j)]\, \Delta x \ , \tag{3}$$

or

$$u_1(i) = \sum_{J=1}^{n} \phi_1\, (p_c - 2p_{F1})\, \Delta x \ . \tag{4}$$

For the case of a Hertzian contact, p_c is the Hertz contact pressure distribution (over a given width) and p_{F1} is the Hertz pressure distribution (over the same width) if Roller 1 were in contact with a rigid flat.

If both rollers were elastic, the total interfacial tangential deflection would be given by:

$$\Delta u = u_1 - u_2 \,, \tag{5}$$

where,

$$u_2 = \sum_{j=1}^{n} \phi_2 \, (p_c - 2p_{F2}) \, \Delta x \tag{6}$$

and,

$$\phi_k \, (i,j) = \begin{cases} \dfrac{-(1+\nu_k)(1-2\nu_k)}{E_k} & i > j \\ + \dfrac{(1+\nu_k)(1-2\nu_k)}{E_k} & i < j \end{cases} \,, \tag{7}$$

if $i = j$, $\phi_k = 0$.

Equations for Hertzian Contact

The contact of cylindrical rollers can be described by the Hertz equations in the following form:

$$p_H = \left[\frac{E}{1-\nu^2} \frac{W'}{2\pi R} \right]^{\frac{1}{2}} \,, \tag{8a}$$

$$b_o = 2 \left[\frac{1-\nu^2}{E} \; \frac{2W'R}{\pi} \right]^{\frac{1}{2}} \,, \text{ and,} \tag{8b}$$

$$p = p_H \sqrt{1 - \left(\frac{x}{b_o} \right)^2} \,, \tag{8c}$$

where,

p_H is the maximum pressure,

b_o is the half contact width,

w' is the load per unit length

$$\frac{1}{R} = \frac{1}{R_1} + \frac{1}{R_2}, \text{ and,}$$

$$\frac{1-\nu^2}{E} = \frac{1}{2}\left[\frac{1-\nu_1^2}{E_1} + \frac{1-\nu_2^2}{E_2}\right]. \tag{8d}$$

It follows from Equations 8a and 8b that:

$$p_H = \left[\frac{E}{1-\nu^2}\,\frac{1}{4R}\right] b_o \,. \tag{8e}$$

Deflection Equation

The Hertzian pressure distribution is given by Equations (8a and 8c) or for Equation 4:

$$p_c = \left[\frac{E}{1-\nu^2}\,\frac{1}{4R}\right] b_o \sqrt{1-\left(\frac{x}{b_o}\right)^2} \,. \tag{9}$$

The pressure distribution for a cylinder and a rigid flat would be:

$$p_{F1} = \left[\frac{2E_1}{1-\nu_1^2}\,\frac{1}{4R_1}\right] b_o \sqrt{1-\left(\frac{x}{b_o}\right)^2} \,. \tag{10}$$

In integral form Equation 4 appears:

$$u_1(i) = \int_{-b_o}^{x} \frac{(1+\nu)(1-2\nu)}{E} (p_c - 2p_{F1})\, dx - \int_{x}^{b_o} \frac{(1+\nu)(1-2\nu)}{E} (p_c - 2p_{F1})\, dx \quad (11)$$

or

$$u_1 = \frac{b_o^2}{R_1} \left(\frac{1-2\nu_1}{1-\nu_1} \right) \left\{ -2 + \left(1 + \frac{R_1}{R_2} \right) \frac{1}{(1+\gamma)} \right\} I , \quad (12)$$

where,

$$\gamma = \frac{E_1}{E_2} \frac{(1-\nu_2^2)}{(1-\nu_1^2)} ,$$

and,

$$I = \frac{x}{b_o} \sqrt{1 - \left(\frac{x}{b_o} \right)^2} + \sin^{-1} \frac{x}{b_o} .$$

A very similar equation could be developed to express the deflection for Roller 2,

$$u_2 = \frac{b_o^2}{R_2} \left(\frac{1-2\nu_2}{1-\nu_2} \right) \left\{ -2 + \left(1 + \frac{R_2}{R_1} \right) \frac{\gamma}{1+\gamma} \right\} I .$$

The slip condition then is given by:

$$\Delta u = u_1 - u_2 . \quad (13)$$

Note if both rollers have identical radii and material properties then:

$$\Delta u = 0 \ . \tag{14}$$

Application to Coated Bodies

Equation 6 is a general equation for computing tangential deflection under normal contacts. The method requires that the pressure distribution between contact surfaces, p_c, and the pressure distributions between a rigid flat and each of the contacting surfaces (p_{F1} and p_{F2}) be known. With these pressure distributions and the appropriate influence coefficients, the tangential deflection can be computed. If, further, the influence coefficients relating deformation to traction is known, the interfacial shear stress can be determined.

Methods for computing the requisite pressure are given in Reference 2. Equations for computing interfacial shear stresses are given in Reference 3. The influence coefficients for relating pressure to tangential deformation and shear stresses are discussed in Appendices A and B.

The pressures are computed by the equation,

$$\sum [\phi_p(i,j) - \phi_p(i,j)] \ p_j \Delta x = \frac{b_o^2 - x_j^2}{2R} \tag{15}$$

where,

$$\begin{aligned} &\phi_p = v - v_1 \text{ (Equation A-19)} \\ &\phi(1,j) = \phi(i,j) \text{ when } x = b, \text{ and} \\ &p_i \text{ is the pressure.} \end{aligned} \tag{16}$$

The slip is computed using Equation 5,

$$\Delta u = \sum [\phi_1 (p_c - 2p_{F1} - \phi_2 (p_c - 2p_{F2})] \Delta x \quad (17)$$

where,

ϕ_1 = u_n (Equation A-25 with $\beta = 0$, and

ϕ_2 = u_n (Equation A-25 with $\beta = 1$ and $s_o = 0$).

The surface shear stress is computed by the equation,

$$\sum \phi_T (i,j) \tau_i \Delta x = \Delta u , \quad (18)$$

where,

$$\phi_T = u - u_1 \text{ (Equation B-11)} . \quad (19)$$

ANALYSES OF SHEAR CONDITIONS IN BALL TESTS

The contact shear stress theory was used to evaluate experimental coating wear data. Elastic properties for the coatings are given in Table 2 (see Reference 4) and the contact stress conditions for uncoated ball-flat contact is given in Table 3. Since analyses are for line contact situations and the experiments were conducted for point contacts, some type of adjustment factor must be used.

The adjustment factor used will involve determining the equivalent nip and local width for (an uncoated) roller on flat that gives the same peak contact pressure as occurs with an uncoated ball on flat. The roller radius was assumed to be the same as the ball radius. For a ball on flat,

$$p_H^3 = 0.059\ PE^2/R^2$$
$$(b_B)^3 = 1.36\ PR/E\ . \tag{20}$$

For a roller on a flat,

$$p_H^2 = 0.175\ \frac{P}{L}\ \frac{E}{R},$$
$$(b_R)^2 = 2.32\ \frac{P}{L}\ \frac{R}{E}\ , \text{ and} \tag{21}$$
$$w' = \frac{P}{L}\ .$$

The equivalent loads and half widths are given in Table 3.

Computation of Shear Stress

With a knowledge of the interfacial deflection it is possible to compute shear stress in the method outlined in Reference 3 and described in Appendix B. Typical shear stress predictions are given in Figures 11 and 12. The concomitant contact pressures are given in Figures 13 and 14 for a coated cylinder in contact with an

TABLE 2. PROPERTIES OF COATINGS

Coating	Modulus of Elasticity	β	Poisson's Ratio	Friction Coefficient
MoS_2	2.5 GPa (362 ksi)	0.012	0.38	0.1
Lead	13.8 GPa (2000 ksi)	0.075	0.45	~ 0.1

TABLE 3. CONTACT CONDITIONS FOR TESTS AND ANALYSES

Case	Ball Load N (lbs)	Contact Pressure GPa (ksi)	Nip Dimension		Equivalent Load (MN/m) (lb/in)
			Ball-Contact Radius mm (in)	Line Contact Half Width mm (in)	
a	15.5 (3.5)	1 (142)	0.087 (0.0034)	0.11 (0.0043)	0.17 (960)
b	28.9 (6.5)	1.2 (175)	0.107 (0.0042)	0.135 (0.0053)	0.25 (1458)
c	35.6 (8)	1.55 (187)	0.114 (0.0045)	0.142 (0.0056)	0.29 (1665)
d	111 (25)	1.9 (273)	0.165 (0.0065)	0.211 (0.0083)	0.62 (3550)
e	267 (60)	2.5 (365)	0.221 (0.0087)	0.279 (0.011)	1.10 (6340)

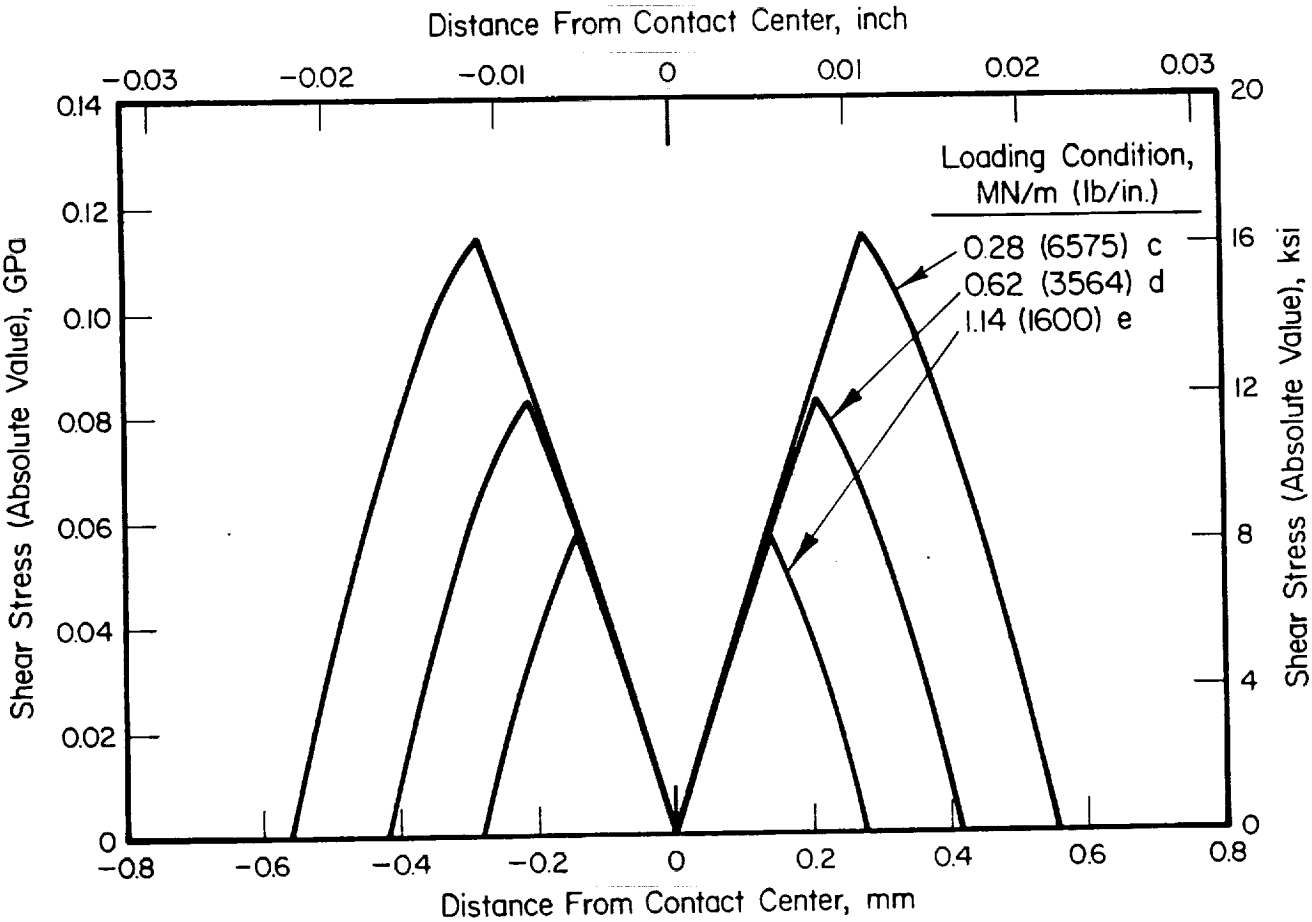

FIGURE 11. PREDICTED SHEAR STRESS DISTRIBUTION UNDER BALL TEST CONDITIONS WITH AN MoS_2 COATING ON BALL

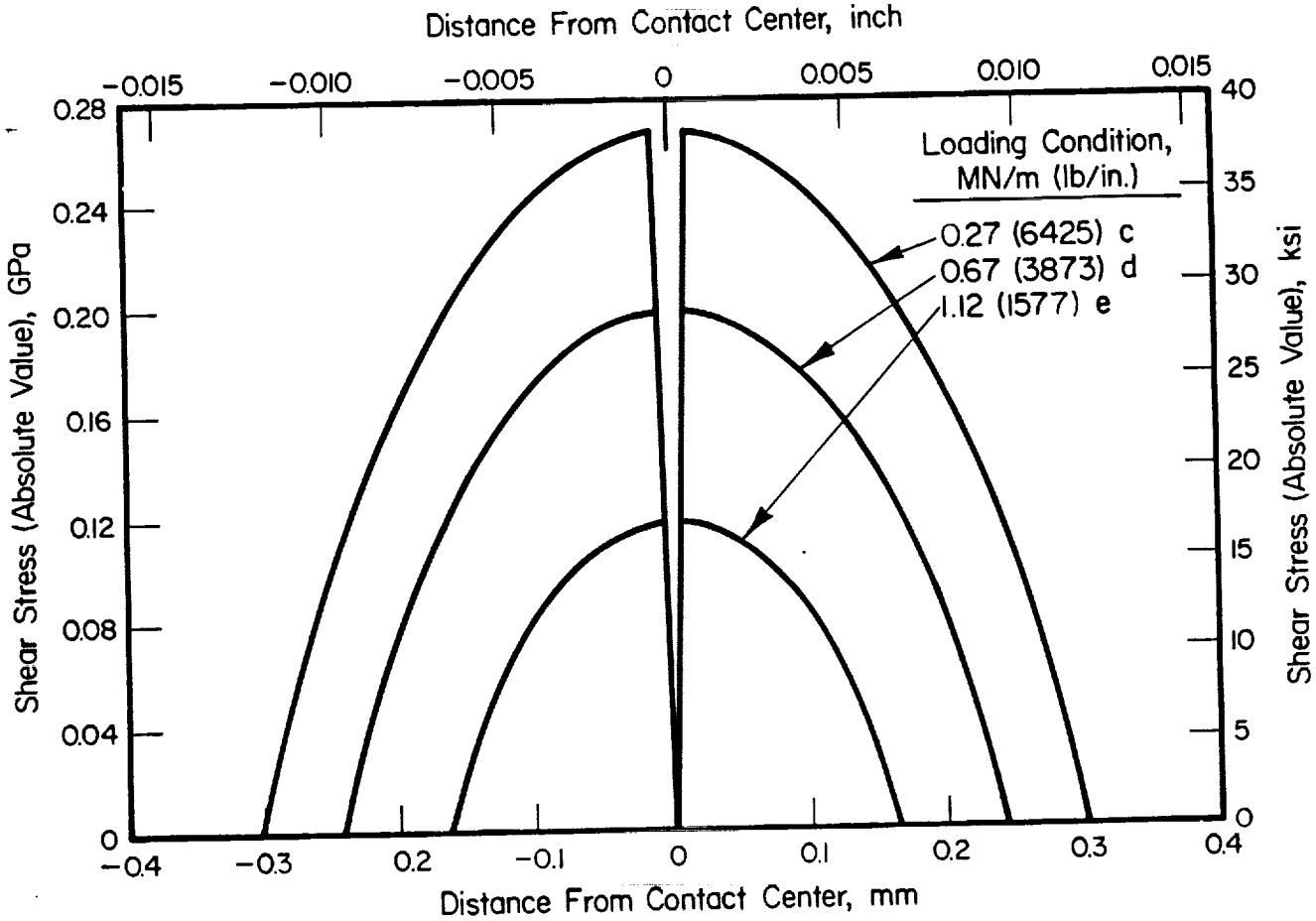

FIGURE 12. PREDICTED SHEAR STRESS DISTRIBUTION UNDER BALL TEST CONDITIONS WITH A LEAD COATING ON BALL

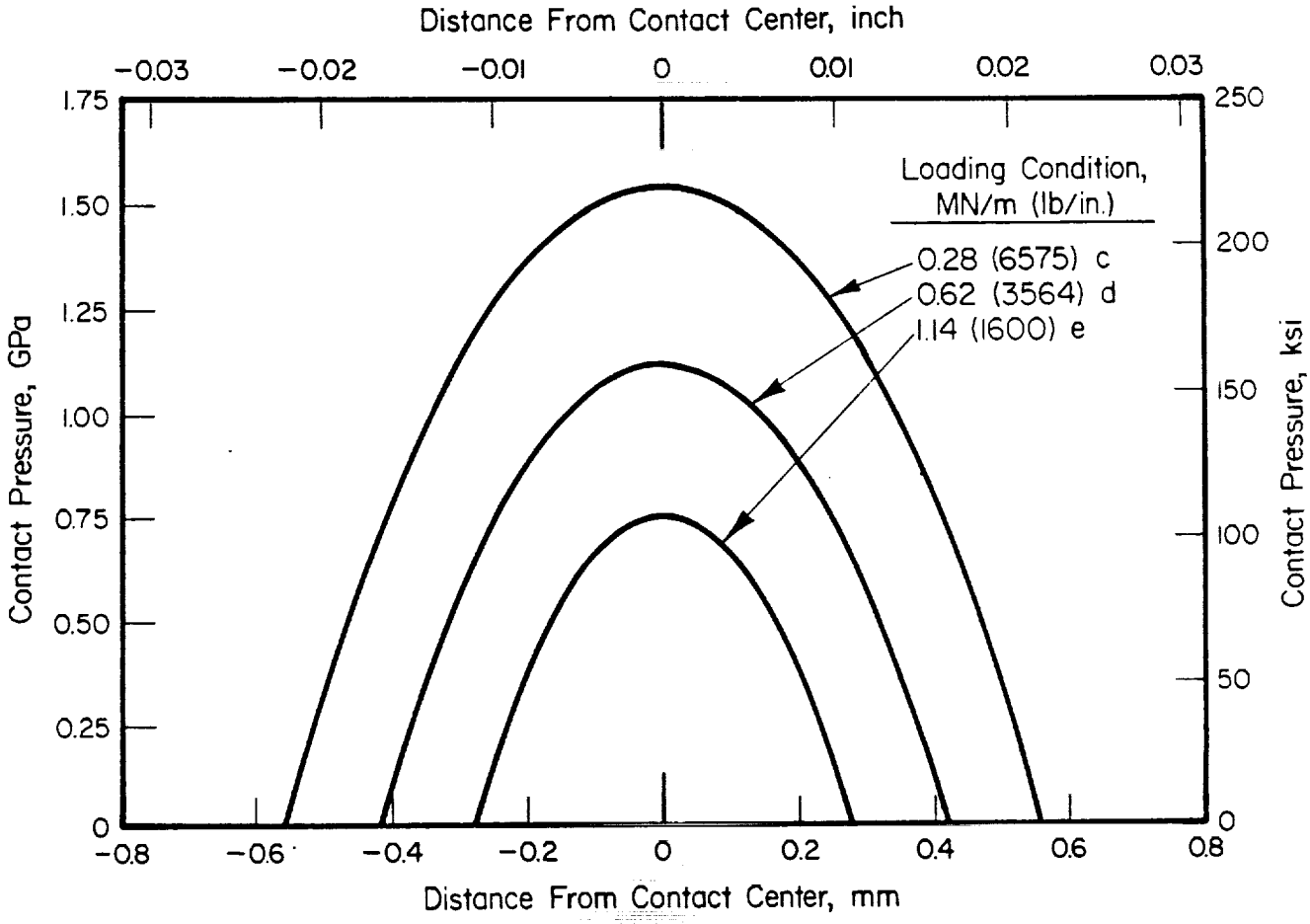

FIGURE 13. PREDICTED NORMAL CONTACT STRESS DISTRIBUTION UNDER BALL TEST CONDITIONS WITH AN MoS_2 COATING ON BALL

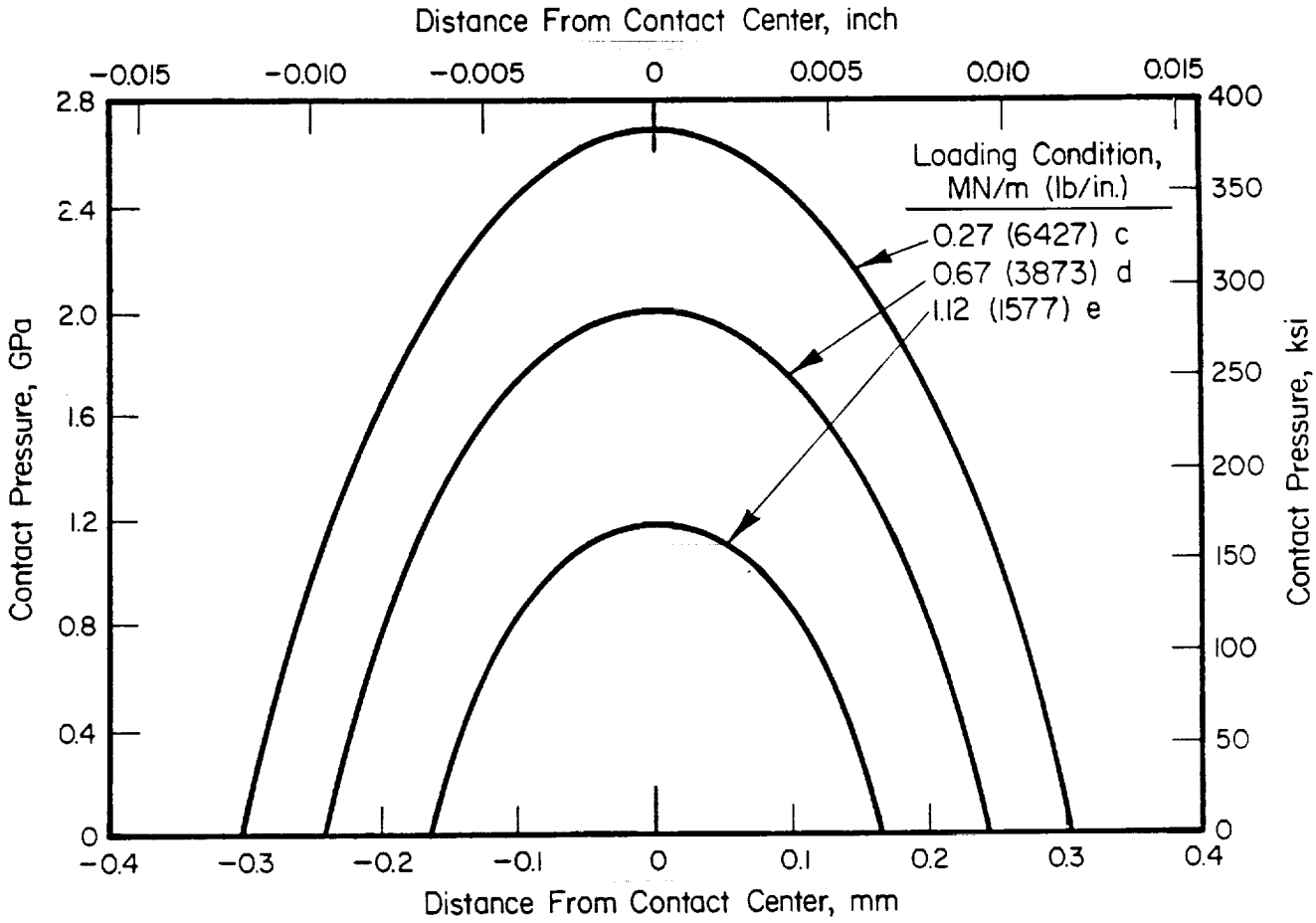

FIGURE 14. PREDICTED NORMAL CONTACT STRESS DISTRIBUTION UNDER BALL TEST CONDITIONS WITH LEAD FILM ON BALL

uncoated flat. Two coatings (MoS_2 and ion plated lead) were analyzed at three loading conditions. The loads were intended to simulate the conditions of Table 3 and the three loads used in the tests.

Surface coatings have a strong influence on interfacial shear stress. The predicted shear stresses were much lower for MoS_2 coated cylinders than for the lead coated cylinders. Also there was a non-slip region for the MoS_2 coating. In the MoS_2 experiments (Figure 5), the non-slip (no-wear) region is clearly seen. For the lead coating experiment, wear (albeit slight) occurs throughout the interface and not just near the edges.

Using the coated ball test data of Figures 7 and 8 it is possible to estimate a coating wear rate factor. Table 4 summarizes the wear factors for different loading and surface roughness conditions. Also given in the table are the estimates of maximum contact stress and interfacial shear stress for the test conditions. If the acceptable wear rates were known, it should be possible to establish acceptable interfacial stress conditions.

Extrapolation To Rolling Contact Lubrication

A ball cyclically loaded against a flat produces interfacial shear stress that resembles the stresses occurring in rolling contact. For example, in both rolling contact and cyclically loaded contact the surfaces are deformed tangentially and create zones of adhesion and of slippage. The primary difference between these two types of loadings is that in a cyclically loaded case deformation of the surfaces are relieved and reimposed for each cycle; whereas for the rolling contact situation new deformations depend on the previous deformations.

In rolling contact theory, the interfacial stresses are not symmetrical about the center of contact (see Figure 15). The stresses tend to be small on the right side of the contact center. Near that at the center of contact the deformations are reversed. At the exit of contact (to the left) stresses are reformed much as stresses are generated by cyclically loading. Predicted stresses for solid bodies in rolling contacts[5] are given in Figure 16.

TABLE 4. AVERAGE MoS_2 COATING LOSS (PERCENT/PER CYCLE)

Load		Roughness		Max. Contact Stress GPa (ksi)	Max. Shear Stress GPa (ksi)	MoS_2 loss rate* (percent/cycle)	Max. Contact Stress GPa (ksi)	Max. Shear Stress GPa (ksi)	Lead Loss Rate** (percent/cycle)
N	lbs	μm	μin						
22.2	8	0.03 to 0.06	(1-2)	0.69	0.06	~0	1.2	0.12	~0
		0.15 to 0.20	(6-8)	(100)	(8)	0.8×10^{-4}	(170)	(17)	
		0.25 to 0.31	(10-12)			1.8×10^{-4}			
111	25	0.03 to 0.06	(1-2)	1.0	0.075	5×10^{-4}	1.9	0.19	6.25×10^{-6}
		0.15 to 0.2	(6-8)	(150)	(11)	3×10^{-4}	(280)	(28)	
		0.25 to 0.31	(10-12)			8×10^{-4}			
266	60	0.03 to 0.06	(1-2)	1.6	0.11	1.7×10^{-4}	2.6	0.26	7×10^{-6}
		0.15 to 0.2	(6-8)	(230)	(16)	4.2×10^{-4}	(380)	(38)	1.7×10^{-4}
		0.25 to 0.31	(10-12)			14×10^{-4}			

*Averaged from measurements at 4, 6, 10, and 20 K cycles

**Based on 120K cycle tests

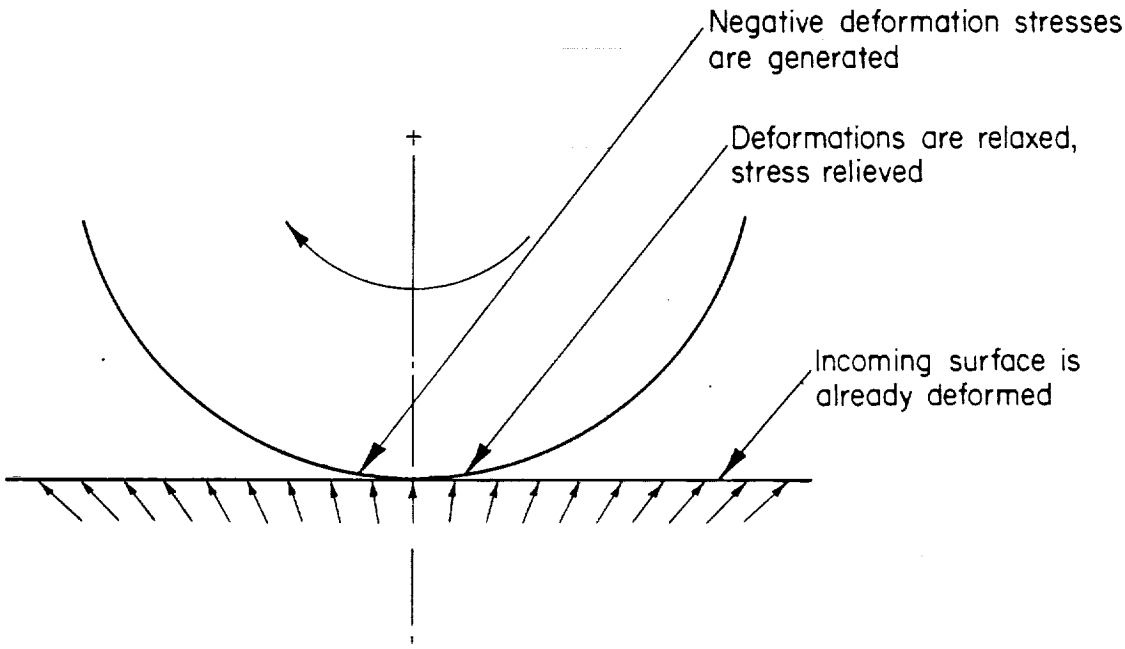

FIGURE 15. MODEL OF SURFACE STRESS FORMATION IN ROLLING CONTACT

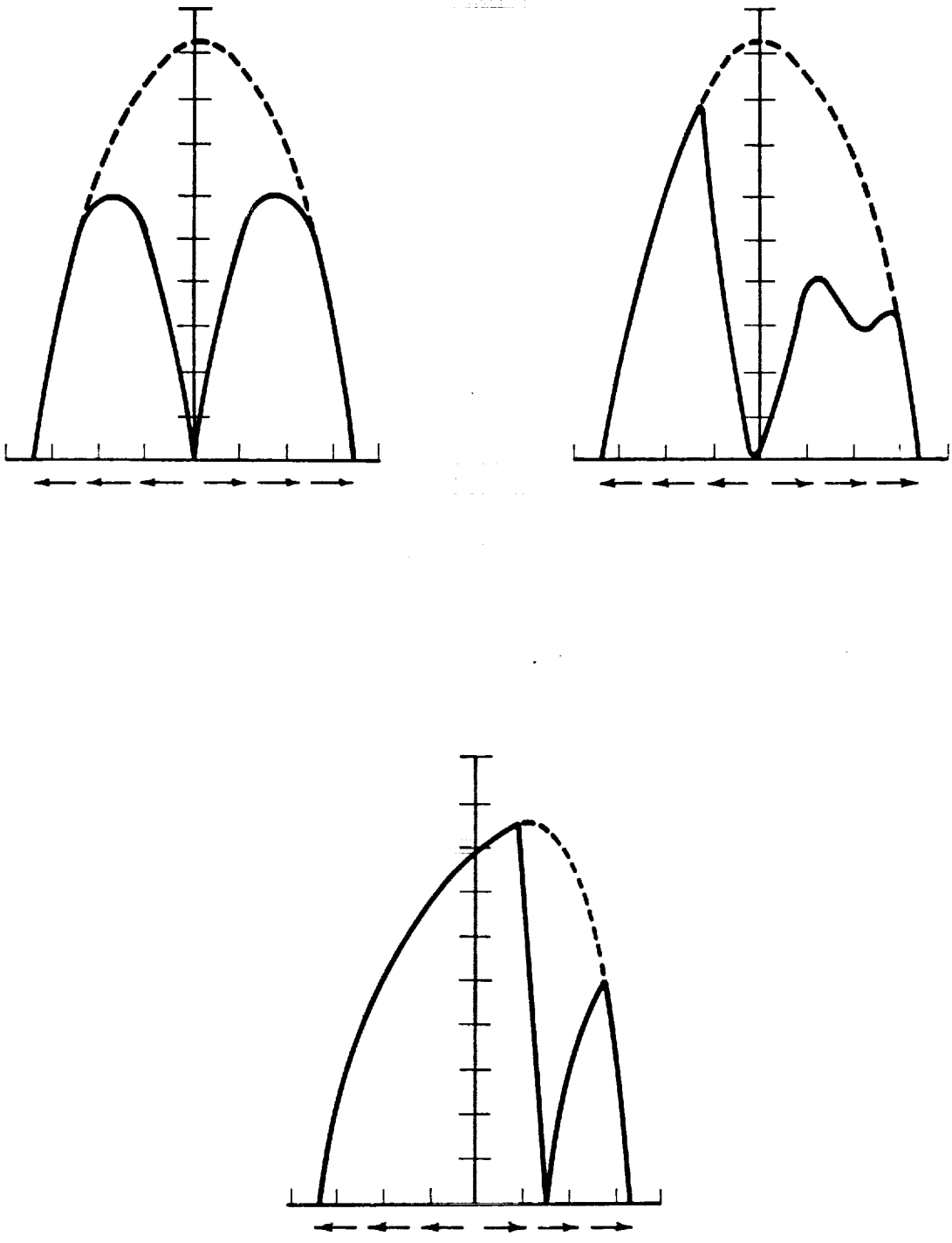

FIGURE 16. CONTACT (SHEAR) STRESSES IN STATIC AND ROLLING CONTACT (KALKER)

When the surfaces are initially pressed into contact, the stress distribution is the same as occurred in the cyclically-loaded ball experiment. As the surfaces roll past each other the stress patterns become unsymmetrical and eventually reach the steady state condition of Figure 16c. Note at these conditions the surface on the left of center are under high shear stresses that occur under cyclic loading.

It seems reasonable to assume the cyclically loaded tests model the exit conditions for rolling contact. Since the exit zone is the only region of high stress, the ball plate tests should reflect the performance life of surface layers in rolling contact.

EVALUATION OF ALPHA AND BETA JOINTS

The computer program ATCON was used to predict contact shear and normal stress for a roller inner race contact of the type described for the Alpha joint. Figures 17 and 18 present shear stress predictions and Figures 19 and 20 present normal stresses. The Alpha joint should operate for about 1.75×10^5 cycles. The rollers must endure on the order of 10^7 cycles. If a target goal is say, 50 percent coating loss maximum, the loss rate must be less than 5×10^{-6} (percent/cycle). Based on the data of Table 4, for an MoS_2 coated surface, the maximum shear stress must be low [< 0.06 GPa (8 ksi)] and the surface must be smooth. For a lead coated surface the stress should be less than about 0.19 GPa (28 ksi) on a smooth surface.

Based on the prediction of Figure 17 it can be seen that the maximum roller load for MoS_2 coated rollers should be less than 1.27 MN/mm (7,000 lb/in.). For a lead coated roller, loads on the order of 2.5 MN/m (14,000 lb/in) may be feasible.

The goal of this research is, of course, not to design an Alpha or Beta joint lubricated bearing but rather to evaluate possible approaches for achieving good performance life. Based on this study, it appears that good life can be achieved by appropriate selection of materials and surface findings. Since specific data were available for the Alpha and not the Beta joint bearing, the analyses have focused on the Alpha joint. However, the same general conclusions regarding reasonable loads, coatings, and surface finish should be applicable for any bearing type.

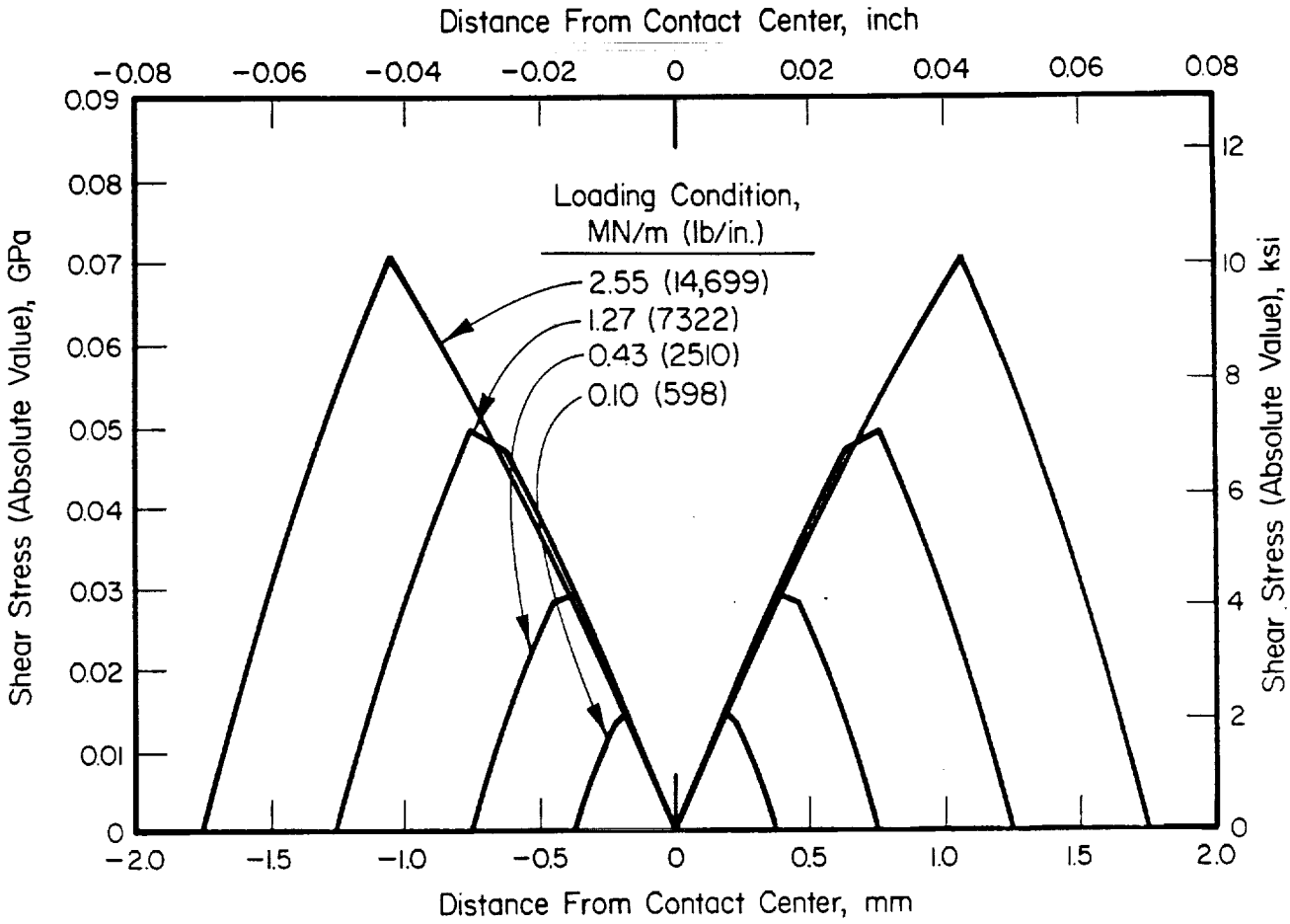

FIGURE 17. PREDICTED CONTACT (SHEAR) STRESS BETWEEN COATED ROLLER AND RAIL AS A POSSIBLE ALPHA JOINT
COATING - MoS_2 5 MICROMETERS (20 μin) THICK
R_{roller} - 0.03 m (1.25 in)

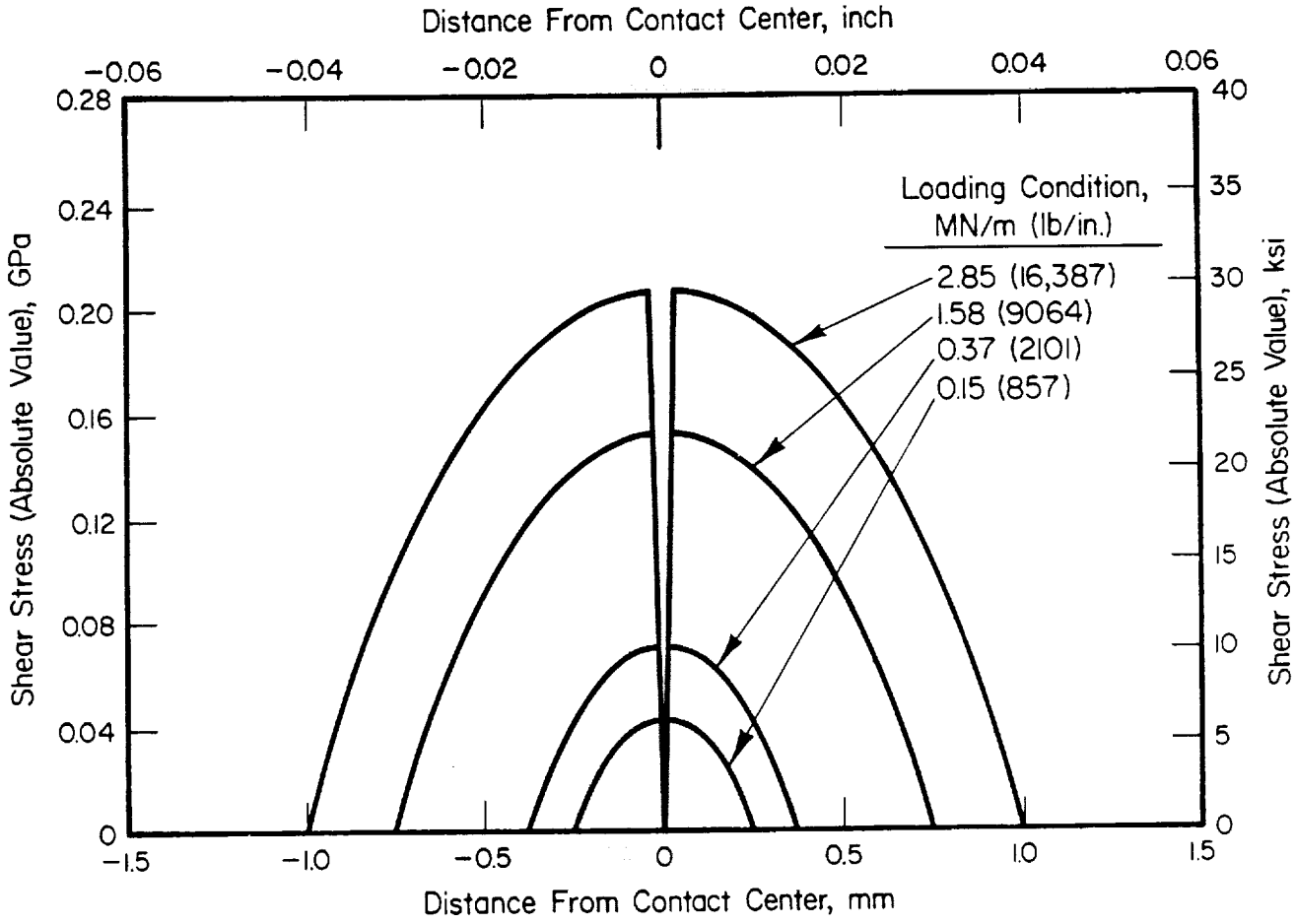

FIGURE 18. PREDICTED CONTACT (SHEAR) STRESS BETWEEN COATED ROLLER AND RAIL IN POSSIBLE ALPHA JOINT
COATING - ION PLATED LEAD
5 MICROMETERS (20 μin) THICK - R_{roller} - 0.03 m (1.25 in)

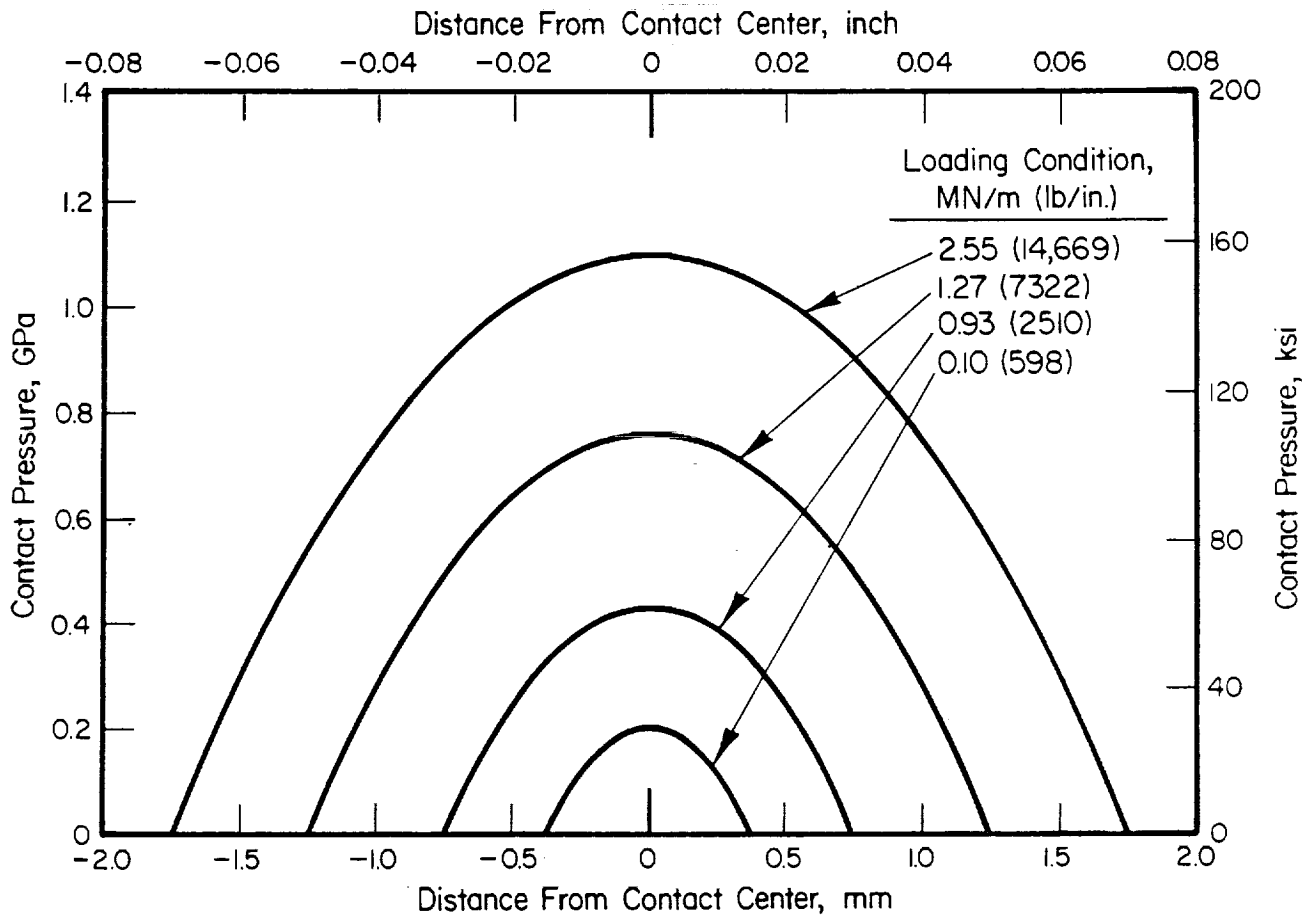

FIGURE 19. PREDICTED CONTACT (NORMAL) STRESS BETWEEN ROLLER AND RAIL IN POSSIBLE ALPHA JOINT COATING - MoS_2 - 5 MICROMETERS (20 μin) THICK R_{roller} - 0.03 m (1.25 in)

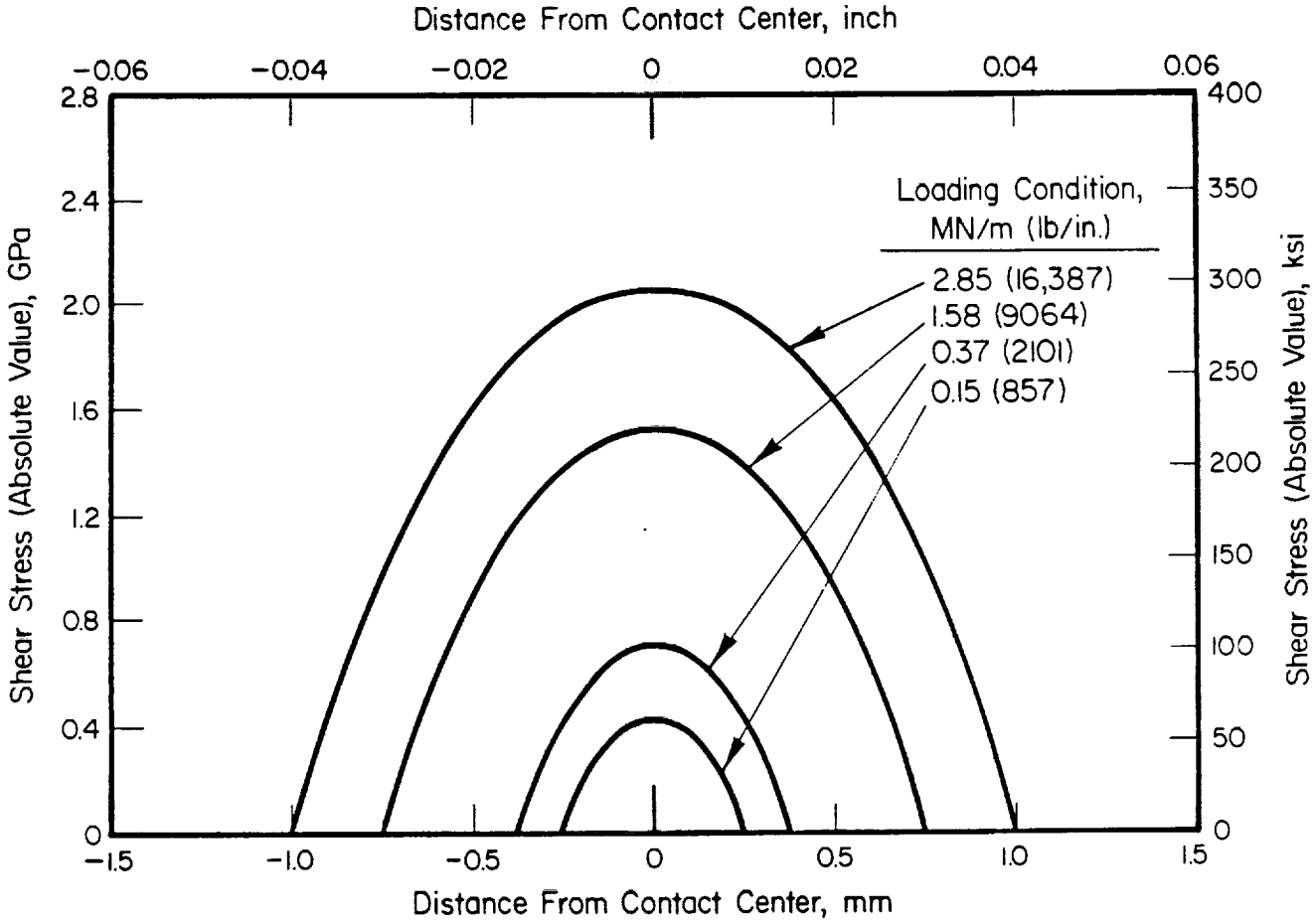

FIGURE 20. PREDICTED CONTACT (NORMAL) STRESS BETWEEN ROLLER AND RAIL IN POSSIBLE ALPHA JOINT
COATING - ION PLATED LEAD
5 MICROMETERS (20 μin) THICK
R_{roller} - 0.03 m (1.25 in)

REFERENCES

1. Poritsky, H., "Stresses and Deflections of Cylindrical Bodies in Contact with Application to Contact of Gears and of Locomotive Wheels", J. Applied Mechanics, v. 17, Trans. ASME, v. 72, 1950, pp. 191-201.

2. Gupta, P.K., and Walowit, J.A., "Contact Stresses Between An Elastic Cylinder and a Layered Elastic Solid", Trans. ASME J.O.T., April 1974, pp 250-257.

3. Kannel, J.W., and Dow, T.A., "Analysis of Traction Forces in a Precision Traction Drive", Trans. ASME Vol. 108, J.O.T., July 1986, pp 403-409.

4. Litmanov, L. Kh, Petrova, L.N., Sentyurinkhina, L.N., Tarasov, A.A., and Tarasov, N.A., "Determination of Elasticity Constants for Solid Lubricating Coatings", Zavod Lab, 1974, Vol. 40, No. 4, pp 457-458.

5. Kalker, J.J. Three-Dimensional Elastic Bodies in Rolling Contact, Kluwer Academic Publishers, London, 1990, pp 234-235.

6. Sneddon, I.N., Fourier Transformations, McGraw-Hill Book Company, 1951.

APPENDIX A. DEVELOPMENT OF PRESSURE-DEFLECTION EQUATIONS

APPENDIX A

DEVELOPMENT OF PRESSURE-DEFLECTION EQUATIONS

Fourier Transform Equation

The objective of this analysis is to develop a relationship between normal stresses and normal and tangential deflections. The analyses are based on classical elasticity theory using the Fourier transform approach given by Sneddon[5] and Gupta and Walowit[1]. These equations are given in the following form (see Figure (A-1).

$$\sigma_y = \frac{\partial^2 \Psi}{\partial x^2} = -\frac{1}{2\pi}\int_{-\infty}^{\infty} \omega^2 \bar{G} \exp(-i\omega x)\, d\omega$$

$$\sigma_x = \frac{\partial^2 \Psi}{\partial y^2} = \frac{1}{2\pi}\int_{-\infty}^{\infty} \frac{d^2\bar{G}}{dy^2} \exp(-i\omega x)\, d\omega$$

$$\tau_{xy} = -\frac{\partial^2 \Psi}{\partial x \partial y} = \frac{1}{2\pi}\int_{-\infty}^{\infty} i\omega \frac{d\bar{G}}{dy} \exp(-i\omega x)\, d\omega \qquad \text{(A-1)}$$

$$v = \frac{1-\nu^2}{2\pi E}\int_{-\infty}^{\infty} \left[\frac{d^3\bar{G}}{dy^3} - \left(\frac{2-\nu}{1-\nu}\right)\omega^2 \frac{d\bar{G}}{dy}\right] \exp(-i\omega x)\, \frac{d\omega}{\omega 2}$$

$$u = \frac{1-\nu^2}{2\pi E}\int_{-\infty}^{\infty} \left[\frac{d^2\bar{G}}{dy^2} + \left(\frac{\nu}{1-\nu}\right)\omega^2 \bar{G}\right] i \exp(-i\omega x)\, \frac{d\omega}{\omega}$$

where Ψ is the Airy stress function which satisfies the biharmonic equation and G is the Fourier transform of Ψ, symbolically

$$\nabla^4 \Psi = 0 \qquad \text{(A-2)}$$

and

$$\bar{G} = \int_{-\infty}^{\infty} \Psi \exp(i\omega x)\, dx \qquad \text{(A-3)}$$

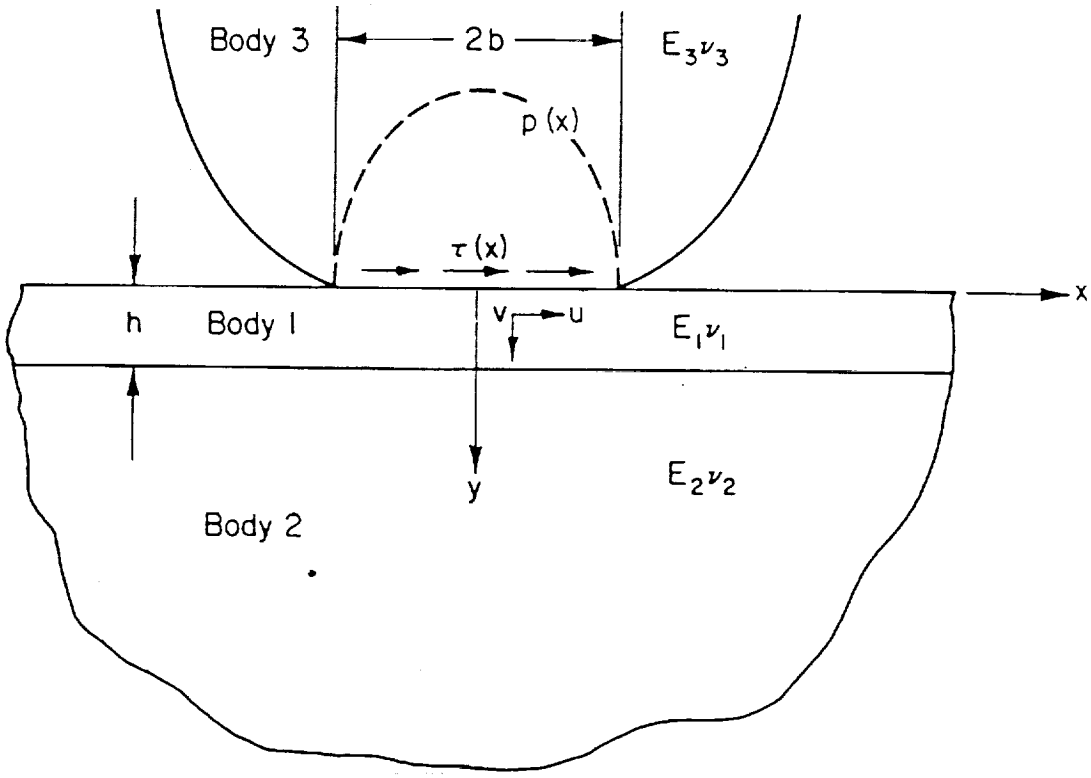

FIGURE (A-1) COORDINATE SYSTEM FOR ANALYSES

Eliminating Ψ from the above two equations and solving the resulting differential equation in $\bar{G}$, we get a solution of the form

$$\bar{G} = (\bar{A} + \bar{B}y) \exp(-|\omega|y) + (\bar{C} + \bar{D}y) \exp(|\omega|y) \tag{A-4}$$

Boundary Conditions

The boundary conditions for the pressure analysis are (assuming no normal pressure)

$$\begin{aligned}
&(\sigma_{y_1})_{y_1=o} = -p(x) && (\tau_{x_1y_1})_{y_1=o} = 0 \\
&(\sigma_{y_1})_{y_1=h} = (\sigma_{y_2})_{y_2=o} && (\tau_{x_1y_1})_{y_1=h} = (\tau_{x_2y_2})_{y_2=o} \\
&(u_1)_{y_2=\bar{h}} = (u_2)_{y_2=o} && (v_1)_{y_1=\bar{h}} = (v_2)_{y_2=o} \\
&(\alpha_{y_2})_{y_2\to\infty} = (\tau_{x_2y_2})_{y_2\to\infty} = 0
\end{aligned} \tag{A-5}$$

Surface Pressure Conditions

Equating the first boundary condition of equation (A-5) with the first of equation (A-1) gives

$$-p(x) = \frac{1}{2\pi} \int_{-\infty}^{\infty} \omega^2 \bar{G} \exp(-i\omega x)\, d\omega \tag{A-6}$$

For $\bar{G}$, even it can be shown that

$$p(x) = \frac{1}{\pi} \int_{o}^{\infty} \omega^2 \bar{G} \cos \omega x\, d\omega \tag{A-7}$$

From Fourier transform theory

$$\omega^2 \bar{G} = \int_{o}^{\infty} p(x) \cos \omega x\, dx \tag{A-8}$$

For a unit loading, assume a loading in the form

$p = 1/\Delta x$ and let $\Delta x \to 0$, so equation (A-8) becomes

$$\omega^2 \bar{G} = \frac{1}{\Delta x} \int_0^{\Delta x} \cos \omega x \, dx = 1 \tag{A-9}$$

letting

$s = h\omega$, $G = \bar{G}/h^2$ and $\eta = y/h$, equation (A-9) becomes

$$s^2 G = 1 \tag{A-10}$$

The surface boundary conditions of pressure and no shear stress can be expressed (using equation (A-4))

$$\begin{aligned} s^2 (A_1 + C_1) &= 1 \\ - A_1 s + B_1 + C_1 s + D_1 &= 0 \end{aligned} \tag{A-11}$$

Note A_1, B_1, C_1, and D_1 refer to the layers while A_2 and B_2 will refer to the substrate.

Remaining Boundary Conditions

The remaining boundary conditions can be met by matching the integrands for each of the conditions of equation (A-5) or

(i) matching normal stresses at the interface

$$(G_1)_{\eta_1=1} = (G_2)_{\eta_2=0} \tag{A-12}$$

(ii) matching shear stresses at the interface

$$(G_1')_{\eta_1=1} = (G_2')_{\eta_2=0} \tag{A-13}$$

(iii) matching normal displacement at the interface

$$\begin{aligned} \frac{1-\nu_1^2}{E_1} \left[G_1''' - \frac{2-\nu_1}{1-\nu_1} s^2 G_1' \right]_{\eta_1=1} \\ = \frac{1-\nu_2^2}{E_1} \left[G_2''' - \frac{2-\nu_2}{1-\nu_2} s^2 G_2' \right]_{\eta_2=0} \end{aligned} \tag{A-14}$$

Finally, matching transverse displacement at the interface

$$\text{(iv)} \quad \frac{1-\nu_1^2}{E_1}\left[G_1'' + \frac{\nu_1}{1-\nu_1}s^2 G_1\right]_{\eta_1=1}$$

$$= \frac{1-\nu_2^2}{E_2}\left[G_2'' + \frac{\nu_2}{1-\nu_2}s^2 G_2\right]_{\eta_2=0} \tag{A-15}$$

The boundary conditions for equations (A-11 to A-15) are summarized in Table A-1.

Green's Function For Normal Deflections

For the case where there is no surface shear ($\bar{G}' = 0$), the fourth equation in the equation set (A-1) can be written

$$v = \frac{1-\nu^2}{\pi E}\int_c^\infty G_1''' \cos\frac{s\zeta}{s^2}\,ds \tag{A-16}$$

where $\zeta = r/h$ is the distance between the unit load and the displacement, and G_1''' is an even function of s. It can be shown that

$$G_1''' = 2(B_1 + D_1)s^2 \tag{A-17}$$

Using a Green's function approach, equation (A-16) can be written

$$v-v_1 = \frac{1-\nu^2}{\pi E_1}\left\{\int_0^\infty 2(B_1+D_1)(\cos s\zeta - \cos s)\,ds - 2\beta \ln\zeta\right\} \tag{A-18}$$

It can be shown for $s \gg 1$ $(B_1 + D_1) \rightarrow 1/s$. Using this condition, equation (A-18) can be written

$$v-v_1 = \frac{1-\nu^2}{\pi E_1}\left\{\int_0^{s_o} 2(B_1+D_1)(\cos s\zeta - \cos s)\,ds + \int_{s_o}^\infty \frac{2(\cos s\zeta - \cos s)}{s}\,ds - 2\beta\ln\zeta\right\} \tag{A-19}$$

TABLE A-1

$$
\begin{bmatrix}
s^2 & 0 & s^2 & 0 & 0 & 0 \\
-z & 1 & z & 1 & 0 & 0 \\
1 & 1 & \bar{t}^2 & \bar{t}^2 & -\bar{t} & 0 \\
-z & 1 - z & z\bar{t}^2 & (1 + z)\bar{t}^2 & z\bar{t} & -\bar{t} \\
z(\nu_1' - 1) & 3 - z - \nu_1'(1 - z) & (1 - \nu_1')z\bar{t}^2 & [2 + (1 + z)(1 - \nu_1')]\bar{t}^2 & (1 - \nu_2')z\bar{t} & (\nu_2' - 1)\gamma\bar{t} \\
(1 + \nu_1'') & (1 + \nu_1'') - 2z/s^2 & (1 + \nu_1'')\bar{t}^2 & [(1 + \nu_1'') + 2z/s^2]\bar{t}^2 & -(1 + \nu_2'')\gamma\bar{t} & 2z\gamma\bar{t}/s^2
\end{bmatrix}
\begin{Bmatrix} A_1 \\ B_1 \\ C_1 \\ D_1 \\ A_2 \\ B_2 \end{Bmatrix}
=
\begin{Bmatrix} 1 \\ 0 \\ 0 \\ 0 \\ 0 \\ 0 \end{Bmatrix}
$$

A-6

where $z = |s|$ $\quad \nu' = (2 - \nu)/(1 - \nu)$ $\quad \beta = (1 - \nu_3^2)E_1/(1 - \nu_1^2)E_3$

$\bar{t} = \exp(z)$ $\quad \nu'' = \nu/(1 - \nu)$ $\quad \gamma = (1 - \nu_2^2)E_1/(1 - \nu_1^2)E_2$

Note if $s_o = o$

$$v-v_1 = \frac{1-\nu_1^2}{\pi E_1}\left\{ \int_o^\infty \frac{2(\cos s\zeta - \cos s)}{s}\, ds - 2\beta \ell n\, \zeta \right\} \qquad (A\text{-}20)$$

or

$$v-v_1 = \frac{-2(1-\nu_1^2)}{\pi E_1}(1-\beta)\ell n\, \zeta$$

which is the equivalent to Poritsky's equation, ~~given in the text as equation (3)~~

Tangential Deflection Due To Unit Normal Load

In the absence of a shear force, the deflection u_n (the last of the A-1 equations) due to a normal load can be written

$$u_n = \frac{1-\nu^2}{2\pi E} \int_{-\infty}^{\infty} \left[G'' + \frac{\nu}{1-\nu} s^2 G \right] i \exp(-i\zeta\eta)\, \frac{ds}{s} \qquad (A\text{-}21)$$

or

$$u_n = \frac{1-\nu^2}{\pi E} \int_o^\infty \left[G'' + \frac{\nu}{1-\nu} s^2 G \right] \frac{\sin s\zeta}{s}\, ds \qquad (A\text{-}22)$$

For larger values of s [4] $A = 1/s^2$ $B = 1/s$ $C_1 = D_1 = 0$

then

$$u_n = \frac{1-\nu^2}{\pi E}\left\{ \int_o^{s_o} \left[G'' + \frac{\nu}{1-\nu} s^2 G \right] \sin\frac{s\zeta}{s}\, ds + \int_{s_o}^\infty \frac{-1+2\nu}{1-\nu} \sin\frac{s\zeta}{s}\, ds \right. \qquad (A\text{-}23)$$

or

$$u_n = \frac{1-\nu^2}{\pi E}\left\{ \int_o^{s_o} \left[G'' + \frac{\nu}{1-\nu} s^2 G + \frac{1-2\nu}{1-\nu} \right] \frac{\sin s\zeta}{s}\, ds - \frac{\pi}{2}\frac{(1-2\nu)}{(1-\nu)} \right\} \qquad (A\text{-}24)$$

Finally,

$$u_n = \frac{1-\nu^2}{\pi E}\left\{ \int_o^{s_o} \left[G'' + \frac{\nu}{1-\nu} s^2 G + \frac{1-2\nu}{1-\nu} \right] \frac{\sin s\zeta}{s}\, ds - \frac{1-2\nu}{1-\nu}\frac{\pi}{2} \right\} \qquad (A\text{-}25)$$

where it is assumed that ν = constant for all materials.

APPENDIX B. DEVELOPMENT OF SHEAR-DEFORMATION EQUATIONS

APPENDIX B

DEVELOPMENT OF SHEAR-DEFLECTION EQUATIONS

The objective of this analysis is to develop a relationship between surface shear stresses and tangential deflections. The analyses are based on the same basic equation as used for the normal stress computations given as equations (A-1 - A-4). The boundary conditions are the same as equation (A-5) with two exceptions as follows:

$$(\sigma_{y_1})_{y_1=o}=0 \quad \text{and} \quad (\tau_{x_1 y_1})_{y_1=o}= -\tau(x) \tag{B-1}$$

Surface Shear Stress Condition

The shear stress solution parallels the normal stress solution in almost all respects. The only exception is a slight difference in the surface stress boundary condition. For the normal stress solution, the shear stress was assumed to be zero and the normal stress was related to the surface pressure. For the shear stress solution, the normal stress is assumed to be zero and the surface shear stress is related to the surface traction. At the surface

$$\tau_{xy}=-\frac{\partial^2 \Psi}{\partial x \partial y} = \frac{1}{2\pi} \int_{-\infty}^{\infty} i\omega \frac{d\bar{G}}{dy} \exp(-i\omega x)\, d\omega$$

If $\frac{d\bar{G}}{dy}$ is an odd function, Sneddon shows that

$$\tau_{xy} = -\frac{1}{\pi} \int_{o}^{\infty} \omega \frac{d\bar{G}}{dy} \cos \omega x \, d\omega$$

Based on Fourier transform theory

$$\omega \frac{d\bar{G}}{dy} = -\int_o^\infty \tau_{xy} \cos \omega x \, dx \tag{B-3}$$

At the surface $y = 0$ $\tau_{xy} = -\tau_o$. Letting τ_o be defined over the interval Δx and letting $\tau_o = 1/\Delta x$ then $\lim_{\Delta x \to o}$ we have

$$\omega \frac{d\bar{G}}{dy} = 1 \tag{B-4}$$

Letting $s = h\omega$ $G = \bar{G}/h^2$ $\eta = y/h$, there results for the first boundary condition

$$s \frac{dG}{d\eta} = 1 \quad \text{for } \eta = o \tag{B-5}$$

Also for the case of no normal stress on the surface

$$G = 0 \tag{B-6}$$

Equations (B-5 and B-6) combine to yield

$$\begin{aligned} A_1 + C_1 &= 0 \\ -A_1 s^2 + B_1 s + C_1 s^2 + D_1 s &= 1 \end{aligned} \tag{B-7}$$

The remaining boundary conditions can be met using the same approach as used for the normal stress conditions (Appendix A). These conditions yield the matrix given in Table B-1.

Green's Function For Shear

The tangential deflection on the surface can be expressed

$$u = -\frac{(1-\nu^2)}{\pi E} \int_o^\infty \frac{d^2G}{d\eta^2} \frac{\cos s\zeta}{s} \, ds \tag{B-8}$$

assuming $\sigma_y = 0$ on the surface. Where

$$\frac{d^2G}{d\eta^2} = -2(B_1 - D_1)\, s \tag{B-9}$$

TABLE B-1

$$
\begin{bmatrix}
1 & 0 & 1 & 0 & 0 & 0 \\
-s^2 & s & s^2 & s & 0 & 0 \\
1 & 1 & \bar{t}^2 & \bar{t}^2 & -\bar{t} & 0 \\
-z & 1 - z & z\bar{t}^2 & (1 + z)\bar{t}^2 & z\bar{t} & \bar{t} \\
z(\nu_1' - 1) & 3 - z - \nu_1'(1 - z) & (1 - \nu_1')z\bar{t}^2 & [2 + (1 + z)(1 - \nu_1')]\bar{t}^2 & (1 - \nu_2')z\bar{t} & (\nu_2' - 3)\gamma\bar{t} \\
(1 + \nu_1'') & (1 + \nu_1'') - 2z/s^2 & (1 + \nu_1'')\bar{t}^2 & [(1 + \nu_1'') + 2z/s^2]\bar{t}^2 & -(1 + \nu_2'')\gamma\bar{t} & 2z\gamma\bar{t}/s^2
\end{bmatrix}
\begin{Bmatrix} A_1 \\ B_1 \\ C_1 \\ D_1 \\ A_2 \\ B_2 \end{Bmatrix}
=
\begin{Bmatrix} 0 \\ 1 \\ 0 \\ 0 \\ 0 \\ 0 \end{Bmatrix}
\qquad \text{B-3}
$$

where $z = |s|$ $\quad \bar{t} = \exp(z)$ $\quad \nu' = (2 - \nu)/(1 - \nu)$ $\quad \nu'' = \nu/(1 - \nu)$.

$\beta = (1 - \nu_3^2)E_1/(1 - \nu_1^2)E_3$ $\quad \gamma = (1 - \nu_2^2)E_1/(1 - \nu_1^2)E_2$

Following the Gupta-Walowit approach, the Green's function for a unit load can be written

$$u - u_1 = \frac{1-\nu^2}{\pi E} \left\{ \int_0^\infty 2(B_1 - D_1)\, s\, \frac{\cos s\zeta - \cos s}{s}\, ds - 2\beta\, \ell n\, \zeta \right\} \quad \text{(B-10)}$$

For larger values of s, $(B_1 - D_1) = 1/s$. Equation (B-10) can be expressed as two integrals $(o<s<s_o)$ and $(s_o<s)$, equation (B-10) becomes

$$u - u_1 = \frac{1-\nu_1^2}{\pi E_1} \left\{ \int_0^{s_o} 2(B_1-D_1)(\cos s\zeta - \cos s)\, ds \right. \quad \text{(B-11)}$$

$$\left. + 2 \int_{s_o}^\infty \frac{\cos s\zeta - \cos s}{s}\, ds - 2\beta\, \ell n\, \zeta \right\}$$

Note: if $s_o = o$.

$$u-u_1 = \frac{1-\nu_1^2}{\pi E_1} \left\{ \int_o^\infty 2\, \frac{\cos s\zeta - \cos s}{s}\, ds - 2\beta \ell n\, \zeta \right\}$$

or (B-12)

$$u-u_1 = -2\, \frac{(1-\nu_1^2)}{\pi E_1}\, (1+\beta)\, \ell n\, \zeta$$

which is the same as Poritsky's equation for non-layered surfaces.